



0016-7037(95)00078-X

Effects of climate on chemical weathering in watersheds

ART F. WHITE and ALEX E. BLUM

US Geological Survey, 345 Middlefield Road, MS 420, Menlo Park, CA 94025, USA

Abstract—Climatic effects on chemical weathering are evaluated by correlating variations in solute concentrations and fluxes with temperature, precipitation, runoff, and evapotranspiration (*ET*) for a worldwide distribution of sixty-eight watersheds underlain by granitoid rock types. Stream solute concentrations are strongly correlated with proportional *ET* loss, and evaporative concentration makes stream solute concentrations an inappropriate surrogate for chemical weathering. Chemical fluxes are unaffected by *ET*, and SiO_2 and Na weathering fluxes exhibit systematic increases with precipitation, runoff, and temperature. However, warm and wet watersheds produce anomalously rapid weathering rates. A proposed model that provides an improved prediction of weathering rates over climatic extremes is the product of linear precipitation and Arrhenius temperature functions. The resulting apparent activation energies based on SiO_2 and Na fluxes are 59.4 and 62.5 $\text{kJ} \cdot \text{mol}^{-1}$, respectively. The coupling between temperature and precipitation emphasizes the importance of tropical regions in global silicate weathering fluxes, and suggests it is not representative to use continental averages for temperature and precipitation in the weathering rate functions of global carbon cycling and climatic change models.

Fluxes of K, Ca, and Mg exhibit no climatic correlation, implying that other processes, such as ion exchange, nutrient cycling, and variations in lithology, obscure any climatic signal. The correlation between yearly variations in precipitation and solute fluxes within individual watersheds is stronger than the correlation between precipitation and solute fluxes of watersheds with different climatic regimes. This underscores the significance of transport-induced variability in controlling stream chemistry, and the importance of distinguishing between short-term and long-term climatic trends. No correlation exists between chemical fluxes and topographic relief or the extent of recent glaciation, implying that physical erosion rates do not have a critical influence on chemical weathering rates.

INTRODUCTION

The intensive interest in past and present global climate change has renewed efforts to quantitatively understand feedback mechanisms between climate and chemical weathering (e.g., Volk, 1987; Berner, 1991, 1994; Brady, 1991; Velbel, 1993a; Brady and Carroll, 1994). During silicate hydrolysis, CO_2 is consumed by release of H^+ from carbonic acid. Over geologic time, such chemical weathering can buffer atmospheric CO_2 , thus moderating large increases and decreases in global temperature and precipitation through the greenhouse effect. The term “weathering” implies that chemical weathering is strongly affected by climate, principally by moisture and temperature (Ollier, 1984). A major uncertainty in present climate models is the sensitivity of weathering rates to these climatic variables. If small changes in climate cause large changes in weathering, the feedback is strong, coupling in the models is tight, and predicted climate variability is limited. If weathering is relatively insensitive to changes in temperature and precipitation, then the feedback is weak and wider excursions in global climate are predicted.

Most of the natural weathering studies (e.g., Meybeck, 1979, 1980; Dunne, 1978; Peters, 1984; Dethier, 1986) used to calibrate the weathering function in climate models have evaluated the effects of precipitation, runoff, and temperature from solute concentrations and fluxes in large scale river systems (10^2 – 10^6 km^2). Attempts (Velbel, 1993a) have been made to discern the interconnection between climate and chemical weathering in smaller scale watersheds and catchments (0.1 – 10 km^2). Although geographically much more limited, such watersheds furnish solute inputs to these larger river systems, and have better defined hydrology and solute budgets. The interpretation of weathering processes in small

watersheds are also less encumbered by regional meteorologic, geologic, biologic, and anthropogenic complexities.

Climatic impacts on chemical weathering must ultimately cause fundamental differences in the thermodynamic and kinetic interactions between minerals and solutions. Quantifying such processes is difficult on a watershed scale. Therefore, most watershed weathering studies have utilized simpler approaches, based on either solute concentrations or fluxes as surrogates for weathering intensity. The most direct approach involves comparison of dissolved solute concentrations as employed by Meybeck (1986) and Drever and Zobrist (1992) in correlating dissolved SiO_2 with elevation and temperatures in European watersheds. The use of chemical fluxes in climatic comparisons overcomes evaporation and dilution effects, which may distort chemical concentrations, but requires additional data on hydrochemical budgets. Regional comparisons of watershed fluxes as functions of annual precipitation and/or runoff include river systems in Kenya (Dunne, 1978) and portions of North America (Dethier, 1986; Peters, 1984). Recently, inorganic carbon fluxes in major river systems produced from weathering of different rock types have been compared (Probst et al., 1992; Amiotte-Suchet and Probst, 1993).

This study tabulates available solute concentration and flux data for a worldwide distribution of watersheds underlain by granitoid rock types. The principal purpose of many of the cited studies was the characterization of acid deposition, deforestation, nutrient cycling, and other issues not directly related to chemical weathering. These watershed studies, representing extensive investments of time and effort, have produced detailed characterization of physical, hydrologic, and chemical processes on a site-specific scale. To the knowledge of the authors, no previous attempt has been made to utilize

this watershed data to evaluate the impact of climate on chemical weathering rates. This paper will attempt such a synthesis and will offer insights into the processes affecting weathering in watersheds, the feedback between climate and weathering, and the implications for global climate models.

METHODOLOGY

Any successful attempt to compare weathering rates based on climatic differences requires physical and hydrologic similarities in the watersheds and a degree of uniformity in measurement and computational approaches. This section describes criteria used for selecting watersheds and the methods used to calculate solute concentrations and fluxes.

Lithology

Lithologic differences may be the dominant factor determining weathering rates in watersheds (Meybeck, 1986; Bricker and Rice, 1989). The relative reactivity of minerals decreases in the order: carbonates > mafic silicates > feldspars > quartz. Attempts to recognize climatic effects in watersheds with grossly different rock types are, therefore, bound to fail. In the following synthesis, only watersheds underlain by predominantly plutonic granitic rocks and high grade metamorphic gneisses are considered. Watersheds draining granites and gneisses are reported by Meybeck (1986) to have similar stream chemistries and weathering rates.

Some watersheds contained limited quantities of nongranitoid lithologies. Watersheds containing small quantities of less reactive rocks, such as quartzites and schists, were included, whereas watersheds containing mafic crystalline rocks, carbonates, and shales were excluded. Overall weathering rates depend not only on the bulk rock mineralogy, but also on the presence of minor mineral phases such as hydrothermal carbonates and sulfides. The presence or absence of trace minerals is generally not reported in the literature (for an exception, see Mast et al., 1990) and present a significant nonclimatic variable in any watershed comparison.

Vegetation

As discussed by Berner (1992) and Stallard (1992), the extent and type of vegetation can have complex effects on chemical weathering rates. The generation of CO₂ and organic acids in the root zone provides hydrogen ions that have been experimentally shown to accelerate silicate hydrolysis. Vegetation also prevents physical erosion, increasing soil depth and age. This may affect weathering rates in a complex manner by decreasing the exposure of fresh bedrock while increasing moisture retention.

The watershed studies in Table 1 are heavily biased toward alpine and forested vegetation that vary from alpine tundra and bare outcrops to coniferous forest, deciduous forest, and one tropical forest site. Grasslands and other ecosystems are under-represented. There is no clear trend that suggests that vegetation systematically influences chemical weathering rates. However, the type and extent of vegetation vary with precipitation and temperature, and any effect of vegetation may be incorporated into the climatic trends.

Temperature

Available temperature data are, generally, mean annual or mean seasonal air temperatures monitored at the stream outlet (i.e., lowest elevation), and these are tabulated in Table 1. When temperatures were measured at significantly different elevations than the outlet, the temperature was adjusted using a thermal gradient of 0.0065°C·m⁻¹. Diurnal and seasonal fluctuations in air temperature are highly attenuated in soils at depths greater than several feet, and mean annual air temperature is a crude but reasonable surrogate for soil temperatures (Velbel, 1993a).

Solute Chemistry

Stream concentrations of Na, K, Ca, Mg, and SiO₂ reflect watershed weathering to various degrees. Daily and seasonal fluctuations in stream chemistry are dependent on complex hydrochemical processes, such as mixing of base and storm flow. Therefore, long-term average concentrations, commonly reported on an annual basis, are required in any climatic comparison. Two averaging techniques were commonly employed in the tabulated watersheds (Table 1). For a number of watersheds, such as Jamieson Creek (Zeman, 1978) and Glendyle (Creasey et al., 1986), grab samples were taken on a weekly or monthly basis. The annual discharge concentration ($C_{i,dis}$) is defined as the arithmetic average of the number of samples q such that (Zeman, 1978)

$$C_{i,dis} = \frac{\sum_{j=1}^q C_{i,j} Q_{i,j}}{Q_t} \quad (1)$$

$C_{i,j}$ is the concentration of an individual stream sample, $Q_{i,j}$ is the stream discharge during the sampling interval from j to $j - 1$, and Q_t is the total annual discharge.

A more fundamental approach for accounting for chemical fluctuations as a function of discharge was developed by Johnson et al. (1969) such that

$$C_{i,dis} = \left[\frac{1}{1 + \beta R} \right] (C_s - C_p) + C_p \quad (2)$$

This model assumes two component solute mixing of a soil water C_s and precipitation C_p . R is runoff and β is an empirical parameter related to soil water volume and fluid residence time. At low runoff, $C_{i,dis}$ approaches C_s and at high runoff, C_p . This expression can be integrated with respect to the simultaneous hydrograph to produce an accurate annual discharge-weighted chemistry. Examples of studies in Table 1 that used this approach are the Hubbard Brook (Likens et al., 1977) and Hanley (Feller and Kimmins, 1984) watersheds. Many watersheds, such as Hubbard Brook and Coweeta (Table 1), have multiyear records extending over decades. For comparisons between watersheds, we used the mean of all available annual data for chemical concentrations and fluxes, precipitation, runoff, and temperature.

Chemical Fluxes

Operationally, the solute discharge flux $Q_{i,dis}$ for a chemical species i in a watershed is

$$Q_{i,dis} = C_{i,dis} \frac{V}{\Delta t} \quad (3)$$

where $C_{i,dis}$ is the chemical concentration (Eqn. 1 or 2), V is the fluid mass, A is the geographic area of the watershed, and t is time. Solute fluxes are reported in a wide variety of units in the literature, but are recalculated to mol·ha⁻¹·y⁻¹ in Table 1. The relationship between solute discharge fluxes (Eqn. 3) and mean solute concentrations then becomes

$$Q_{i,dis} (\text{mol} \cdot \text{ha}^{-1} \cdot \text{y}^{-1}) = C_{i,dis} (\mu\text{M}) \frac{R (\text{mm})}{100} \quad (4)$$

where R is the annual runoff normalized to watershed surface area (ha) and time (y).

The mass balance used to determine the chemical weathering flux in a watershed can be operationally defined for a chemical species i by the relationship

$$Q_{i,w} = Q_{i,dis} - Q_{i,wet} + Q_{i,bio \text{ uptake}} - Q_{i,decay} + Q_{i,sorp} - Q_{i,desorp} \quad (5)$$

where

$Q_{i,w}$ = net output flux due to chemical weathering from soils and bedrock.

$Q_{i,dis}$ = total discharge flux.

$Q_{i,wet}$ = input flux based on wet precipitation.

$Q_{i,dry}$ = input flux based on dry deposition from aerosols

$Q_{i,\text{bio uptake}}$ and $Q_{i,\text{decay}}$ = uptake flux by biomass and input flux from biological decay

$Q_{i,\text{sorp}}$ and $Q_{i,\text{desorp}}$ = uptake flux by sorption and input flux from desorption in soils and rock

The chemical weathering flux $Q_{i,w}$ can be calculated for a watershed if the fluxes on the right side of Eqn. 5 can be determined. Other potential fluxes not included in Eqn. 5, such as groundwater and anthropogenic inputs from agriculture and road salt, are assumed to be negligible. The discharge flux $Q_{i,\text{dis}}$ is calculated from the mean discharge compositions (Eqn. 1 or 2) and discharge volume measured in a weir or flume at the base of a watershed.

Numerous studies have documented that a significant proportion of solutes ultimately discharged from a watershed are derived from wet $Q_{i,\text{wet}}$ and dry $Q_{i,\text{dry}}$ atmospheric deposition. Precipitation scavenging of aerosols is the primary mechanism for wet deposition, while dry deposition includes sedimentation, aerosol impaction, and gaseous absorption processes (e.g., Swank and Waide, 1988). In the tabulated watersheds (Table 1), atmospheric deposition $Q_{i,\text{precip}}$ was most commonly measured in precipitation collectors open to both wet and dry deposition. Such systems are generally effective in estimating $Q_{i,\text{wet}}$, but generally underestimate $Q_{i,\text{dry}}$, due to an inability to measure aerosol interception and scavenging in the forest canopy. Operationally, a mass balance for total atmospheric input $Q_{i,\text{input}}$ is

$$Q_{i,\text{input}} = [Q_{i,\text{wet}} + \alpha Q_{i,\text{dry}}]_{\text{precip}} + (1 - \alpha) Q_{i,\text{dry}}^*, \quad (6)$$

where α is the efficiency factor by which the precipitation sampler measures dry deposition ($Q_{i,\text{precip}} = Q_{i,\text{wet}} + \alpha Q_{i,\text{dry}}$). "Excess" dry deposition $Q_{i,\text{dry}}^*$ is that not measured by the precipitation collector. Three approaches have been commonly used to correct for excess dry deposition: (1) direct measurement via atmospheric filter packs or other flow through samplers, (2) concurrent measurement of stem-flow and throughfall from forest canopies, and (3) solute ratios based on atmospherically dominated species such as chloride. The first two methods have been applied only to a limited number of watersheds, and involve considerable uncertainties.

The third method is based on the assumption that all the Cl discharge flux originates from atmospheric sources and none from rock weathering. This is a reasonable assumption, considering the low Cl concentrations in granitic rocks (~185 ppm; Garrels and Mackenzie, 1971). The excess dry deposition is then estimated based on whether the atmospheric Cl originated from either terrestrial or marine sources. As developed by Wright and Johannessen (1980) for the Birkenes watershed, nonmarine and marine dry deposition fluxes can be defined, respectively, as

$$Q_{i,\text{dry}}^* = \left[\frac{C_i}{C_{\text{Cl}}} \right]_{\text{precip}} (Q_{\text{Cl},\text{dis}} - Q_{\text{Cl},\text{precip}}) \quad (7)$$

and

$$Q_{i,\text{dry}}^* = \left[\frac{C_i}{C_{\text{Cl}}} \right]_{\text{sea}} (Q_{\text{Cl},\text{dis}} - Q_{\text{Cl},\text{precip}}). \quad (8)$$

Equation 7 assumes that the dry deposition has the same chemical composition as the wet deposition. The difference between measured outputs and inputs is due solely to the efficiency of the precipitation collector (α) in measuring interception and scavenging. This approach is the most practical method for estimating dry fluxes dominated by terrestrial sources. Equation 8 assumes that dry deposition represents marine aerosols and that the dry input composition of other chemical species occurs in the same proportions as that of seawater.

For specific aerosols, the progression from marine-dominated to terrestrial-dominated solutes occurs in the order $\text{Cl} > \text{Na} > \text{K} \gg \text{Mg} > \text{Ca} > \text{SO}_4$ (Berner and Berner, 1987). Ogden (1980), Stallard and Edmond (1983), and others have demonstrated that, while the absolute ionic concentrations of marine aerosols decrease rapidly as a function of distance from the coast, the relative ionic ratios of such aerosols remain relatively constant. For such conditions, Eqn. 8 is the most accurate approach for estimating excess dryfall. For chemical species such as SO_4 which are dominated by terrestrial sources, Eqn. 7 generally produces more accurate dryfall fluxes.

Based on the above approaches, the weathering fluxes for a specific cation i in the watershed Table 1 are calculated from the expression

$$Q_{i,w} = Q_{i,\text{dis}} - Q_{i,\text{precip}} - \left[\frac{C_i}{C_{\text{Cl}}} \right]_{\text{sea}} (Q_{\text{Cl},\text{dis}} - Q_{\text{Cl},\text{precip}}). \quad (9)$$


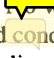
The extent to which the dry deposition correction influences calculated weathering fluxes is determined by the Cl balance in the watershed. If the difference between the Cl discharge flux and the precipitation input is small, then dry deposition is adequately represented by precipitation ($\alpha = 1$, Eqn. 6). If Cl is not balanced, then the total atmospheric input for a solute species is corrected by assuming that the dry deposition has seawater ratios (ratios from Krauskopf, 1967). Silica input is generally not included in precipitation analyses and, when reported, concentrations are very low. Therefore, tabulated SiO_2 weathering fluxes are assumed equal to the discharge fluxes ($Q_{i,w} = Q_{i,\text{dis}}$), and are unaffected by atmospheric deposition.

The above computations do not account for any net biological or ion exchange fluxes in watersheds. The biological flux $Q_{i,\text{bio}}$ of nutrients such as Ca, Mg, and K in Eqn. 5 can be negative in a degrading ecosystem as biomass decomposes, or positive in an aggrading ecosystem as biomass sequesters nutrients. This biological term is considered quantitatively in only a limited number of watershed weathering budgets (e.g., Likens et al., 1977; Stauffer and Wittchen, 1991; Velbel, 1994). The net biological flux is assumed to be zero in the present synthesis.

The exchange flux $Q_{i,\text{exch}}$ (Eqn. 5) can represent net desorption or sorption of cations and anions between soil waters and ion exchange sites, principally on clay and ferric oxyhydroxide minerals. In a geologic time frame, the net flux should be positive due to the progressive formation of these minerals and the increasing exchange capacity of the soil profile. However, for annual watersheds budgets at steady-state, the net flux due to ion exchange should approach zero. This is because ion exchange reactions are much more rapid than chemical weathering, and therefore, closer to equilibrium (Cresser and Edwards, 1987). However, for disturbed watersheds, such as those impacted by acid deposition, sorbed species represent very large chemical reservoirs not at steady-state. When released, sorbed species can significantly affect base cation outputs from a watershed and alter the apparent weathering rate (Eqn. 5). As with the biological component, the lack of quantitative data and methodologies to compute exchange fluxes introduces significant nonclimatic variability in watershed comparisons which is difficult to systematically evaluate.

RESULTS

Tabulation of Watershed Data

Sixty-eight watersheds meeting the preliminary hydrochemical and geologic criteria discussed earlier are tabulated in Table 1. As indicated from the global distributions shown in Fig. 1, the watersheds in Table 1 are geographically limited, with all but four sites in Europe or North America. The watersheds generally encompass alpine to temperate climatic conditions. Weathering of granitoid rocks under tropical conditions is reported only for the Rio Icacos watershed in the El Verde  forest in Puerto Rico (McDowell and Asbury, 1994).  watershed studies typify chemical weathering under arid conditions. Clearly, for an adequate representation of global climate, a more world-wide distribution of watersheds would be desirable, but is presently unavailable. In spite of such limitations, the tabulated watersheds do encompass significant climate differences. Annual precipitation ranges between 620 and 4500 mm·y⁻¹, runoff between 90 and 3700 mm·y⁻¹ and mean annual temperature from -3 to 22°C.

Runoff vs. Precipitation

The relationship between precipitation and runoff is important in evaluating climatic effects on solute chemistry. Although precipitation is the primary climatic variable, mean

Table 1. Chemical, climatological and physical characteristics of watersheds on granitoid rocks. Fluxes are for bulk precipitation Q_{prec} and discharge Q_{dis} and are reported as $\text{mol}\cdot\text{ha}^{-1}\cdot\text{yr}^{-1}$. Temperatures are mean annual air values generally at the watershed outlet. pHs are discharge-weighted averages. Elevations are in meters.

Watershed	Reference ¹	Rock ²	Area (ha)	Elev. min	Elev. max	precip (mm)	runoff (mm)	ET (%)	Temp (°C)	pH	Na Q_{prec}	K Q_{prec}	Ca Q_{prec}	Mg Q_{prec}	Si Q_{dis}	Cl Q_{prec}	SO ₄ Q_{dis}
Canada																	
Exner Lake	Allan et al., 1993	gr	7	na	na	508	225	55	2.4	4.6	29	55	14	63	48	21	40
Hanley A. B. C.	Feller and Kimmins, 1984	dia/grdio	23	140	450	2146	1010	53	9.2	6.70	178	547	20	38	85	411	33
Hanley B.B.C.	Feller and Kimmins, 1984	dia/grdio	68	140	450	2146	1240	42	9.2	6.70	195	616	23	64	95	554	37
Hanley C. B.C.	Feller and Kimmins, 1984	dia/grdio	44	140	450	2146	1040	52	9.2	6.70	200	526	23	41	97	541	37
Jamieson Ck. B. C.	Zeman, 1975	gr/meta	299	304	1280	4541	3668	19	3.4	6.39	572	1113	22	65	181	1039	91
Rawson Lake E. Ont.	Schlinder et al., 1976	gr	170	220	300	803	277	66	2.4	6.00	na	121	na	11	na	87	na
Rawson Lake NE. Ont.	Schlinder et al., 1976	gr	10	220	300	803	277	66	2.4	6.00	68	167	48	82	283	314	38
Rawson Lake NW. Ont.	Schlinder et al., 1976	gr	62	220	300	803	277	66	2.4	6.00	68	116	48	56	283	304	38
Czechoslovakia																	
Hartvík	Paces, 1985	gn/atx	98	724	744	781	467	40	6.0	6.84	48	187	2	25	125	75	28
Salacova Lhota	Paces, 1986	gn/atx	168	567	74	685	128	81	6.5	7.14	40	178	20	30	102	147	26
Vocadlo	Paces, 1986	gn/atx	59	570	635	736	171	77	6.5	6.15	36	413	18	82	95	593	27
Finland																	
Liihapiira	Lepistö et al., 1988	gn	165	42	92	766	480	37	na	6.10	73	193	26	42	70	160	18
Yli-Kruutila	Lepistö et al., 1988	gn	7	42	92	750	198	74	na	6.10	216	234	41	59	185	270	51
France																	
Strengbach	Probst et al., 1992	gr/gn	80	883	1146	1153	1051	32	6.0	na	na	na	na	na	na	na	na
Pont Donar	Bouchard, 1983	gr	24	50	na	976	379	61	na	na	na	3379	na	74	na	117	na
Germany																	
Bärhald	Stahr et al., 1980	gr	na	1000	3000	2000	1395	30	na	na	243	739	51	138	100	424	27
Schluchsee	Feger et al., 1990	gr	11	1150	1250	2300	1974	14	5.0	na	74	1156	53	285	135	519	41
Japan																	
Kiryu	Shimada et al., 1993	gr	6	190	350	1672	936	44	12.6	na	234	2644	66	595	266	580	106
Tsukuba	Hirata & Muraoka, 1993	gr	67	200	380	1587	720	55	13.1	6.85	405	1771	116	168	301	651	177
Norway																	
Bitenes	Wright & Johannessen, 1980	gr	41	200	300	1637	1310	20	5.8	4.62	683	1385	60	67	68	312	95
Bofnane	Skarveit, 1981	gn	340	180	650	3195	na	na	7.5	4.65	2780	3259	61	72	112	288	415
Breidvikdalen	Skarveit, 1981	gn	189	295	695	2910	3712	28	7.5	4.69	2760	3021	96	128	87	189	334
Dyrdalen	Skarveit, 1981	gn	330	438	806	3050	3305	-8	7.5	5.30	3750	3445	92	336	107	549	458
Kaarvatn	Lydersen, 1994*	gn/atx	2500	200	1375	2252	1899	16	5.2	7.00	112	342	39	58	46	190	99
Langfjern	Wright, 1983	gn/gr	5	510	750	852	603	29	3.1	4.85	64	144	26	24	29	162	11
Sogndal 1	Frogner, 1990	gr	na	900	na	984	875	11	na	5.80	389	418	88	33	27	81	38
Sogndal 2	Frogner, 1990	gr	na	900	na	959	870	9	na	5.70	379	393	54	33	27	81	37
Storgama	Lydersen, 1994*	gr	60	580	690	1192	923	23	7.1	4.52	163	285	19	13	31	150	23
Rhodesia																	
Juliadale	Owens & Watson, 1979	gr	910	1800	2000	1220	400	67	13.8	na	na	na	na	na	na	na	na
Rusape	Owens & Watson, 1979	gr	7330	1500	1600	922	87	91	17.1	na	na	na	na	na	na	na	na
Spain																	
Manisany Mtns	Avila and Roda, 1988	sch	430	700	1035	910	na	na	9.0	7.44	291	1065	36	41	474	479	74

na = not available; sch = schist; * = unpublished data.

Only the principal literature sources are cited. Supplemental information was supplied from programmatic summaries, reports in review, or from personal communications that are acknowledged at the end of the text.

Rock type: *dio* = diorite; *gr* = granite; *gdi* = granodiorite; *meta* = metasediments; *mon* = monzonite; *sch* = schist; *qtz* = quartzite.

Data from personal communication

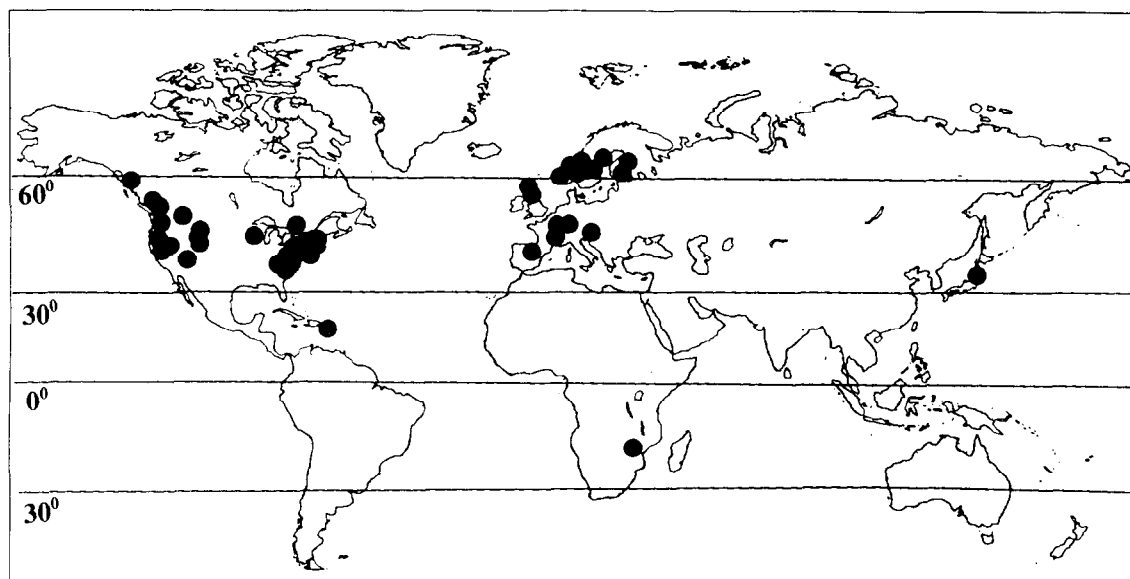


FIG. 1. Geographic distributions of watersheds tabulated in Table 1.

solute concentrations and fluxes are weighted with respect to runoff (Eqns. 1, 2, 4). In a hydrologically closed watershed, runoff (R) and precipitation (P) are related by the expression

$$R = P - ET \quad (10)$$

where ET is the evapotranspiration ($\text{mm} \cdot \text{y}^{-1}$).

Precipitation and runoff for watersheds with alpine/temperate climates (all the watersheds in Table 1 except Rio Icacos) are plotted as the closed symbols in Fig. 2. The Rio Icacos, with additional precipitation and runoff data from tropical watersheds tabulated by Bruijnzeel (1990), are plotted as open symbols in Fig. 2. The majority of both temperate/alpine and tropical watersheds have precipitation and runoff

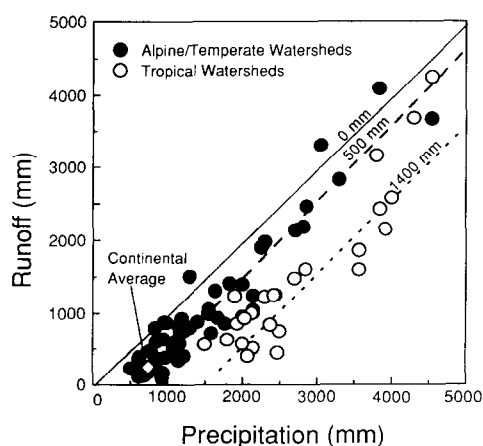


FIG. 2. Correlation between watershed runoff and precipitation for temperate/alpine (●) and tropical (○) watersheds. Solid line assumes a direct correspondence between precipitation and runoff indicative of zero evapotranspiration (ET). Dashed and dotted lines are linear regression fits to temperate/alpine and tropical data with corresponding average ET s. Average world continental precipitation and runoff is indicated by (◇).

greater than the global continental averages ($740 \text{ mm} \cdot \text{y}^{-1}$ and $250 \text{ mm} \cdot \text{y}^{-1}$; Berner and Berner, 1987). This difference reflects that research watersheds usually enclose topographic relief and occur at higher elevations than the average continental land masses. Studies also focus on watersheds with perennial runoff, statistically favoring wet climates.

The alpine/temperate and tropical watersheds produce linear relationships between precipitation and runoff. As expected, the lower temperature alpine/temperate watersheds have a higher runoff to precipitation ratio (less ET) than the warmer tropical watersheds. However, tropical watersheds with very high precipitation, such as Rio Icacos (Table 1), also have lower ET , possibly reflecting the high humidity of these extremely wet environments. The solid diagonal line (Fig. 2) denotes a direct correlation between runoff and precipitation. Most runoff falls below this line denoting water loss by ET (Eqn. 10). However, runoff from several watersheds plot above this line (Breidvkdde, Dyrdaalen, Martinell; Table 1) implying extraneous recharge from groundwater or glacial ablation, or underestimation of precipitation in the watershed. Linear regressions between runoff and precipitation are denoted by the dashed line for the alpine/temperate data ($R = -535 + 1.04P_{\text{(temperate)}}$; $r^2 = 0.90$) and by the dotted line for the tropical data ($R = -1425 + 1.05P_{\text{(tropical)}}$; $r^2 = 0.82$). These regressions indicate that the proportionality between runoff and precipitation approaches unity (i.e., slopes = 1.04 and 1.05, respectively), implying that the absolute ET loss ($\text{mm} \cdot \text{y}^{-1}$) is generally independent of the annual precipitation (Eqn. 10). Within the alpine/temperate data, there is a modest correlation between temperature and ET ($r^2 = 0.30$; $P = 0.002$).

Average ET can be estimated from the intercepts of the alpine/temperate and tropical data trends (500 and 1400 mm, respectively). Relatively constant ET occurs because generally high annual precipitation in the watersheds exceeds the potential ET . In such cases, ET is dependent on the temperature and humidity but not strongly dependent on total pre-

10-11 precipitation will be less than the potential ET , and runoff will approach zero except during heavy precipitation events. Therefore, ET should be strongly dependent on the amount of precipitation. The world continental average ET is 490 mm (Berner and Berner, 1987), near the mean ET of the alpine/temperate watersheds (Fig. 2).

Solute Concentrations vs. Precipitation, Runoff, and ET

Volume weighted mean solute concentrations can be calculated from the discharge fluxes in Table 1 using Eqn. 4. Results indicate that SiO_2 , Na, Mg, and Ca concentrations in alpine/temperate watersheds with high precipitation and runoff are significantly lower than in similar watersheds with low precipitation and runoff (Fig. 3). The only exceptions are watersheds along coastal areas such as Scotland and Norway that receive both high precipitation and large inputs of Na from marine aerosols. In individual watersheds, decreases in solute concentration with runoff are commonly attributed to increased dilution of base flow chemistry by storm flow (Eqn. 2). An alternative, often unrecognized explanation, is that increasing solute concentrations with decreasing precipitation and runoff results from the concentration effects of ET .

The linear precipitation/runoff ratios (Fig. 2) indicate that, although the absolute water loss from ET in the alpine/temperate watersheds is relatively constant, the proportions of ET relative to precipitation is not, and the % ET is much higher

in watersheds with less precipitation than in watersheds with high precipitation. Evaporative water loss can increase chemical compositions by concentration such that

$$C_{i,dis} = C_i^0 \left(\frac{P}{P - ET} \right) \quad (11)$$

C_i^0 is the initial concentration prior to ET . The term in parentheses is equal to the ratio of P to R (Eqn. 10) and can be calculated from the data in Table 1.

Trends of increasing concentrations of SiO_2 , Na, Mg, and Ca with increasing % ET (Eqn. 11) are shown as lines extending upwards from initial values of C_i^0 in Fig. 4. The projected initial concentrations can be up to an order of magnitude more dilute than the mean annual concentrations in high % ET watersheds. The envelope defining these initial concentrations are also plotted as horizontal dashed lines in Fig. 3. The mean annual concentrations in most watersheds fall above these lines indicating significant influence of ET , particularly at low precipitation sites.

Solute Fluxes

Weathering fluxes are calculated for the major cations and SiO_2 using Eqn. 9 and the input and discharge fluxes tabulated in Table 1. Figure 5 shows the relative proportions to which chemical weathering, precipitation, and excess dryfall contribute to total Na discharge fluxes. Each bar represents a single watershed, arranged in order of increasing precipitation

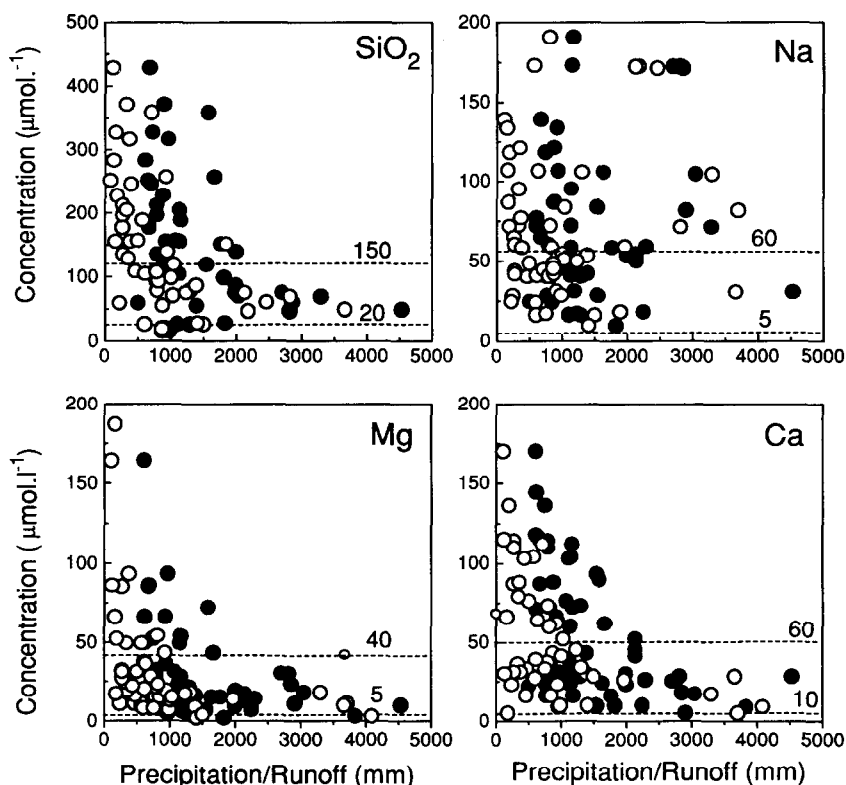


FIG. 3. Solute concentration vs. precipitation (●) and runoff (○). Dashed lines correspond to preevaporative solute concentrations defined by C_i^0 (Eqn. 11). Watershed solutes plotting above these lines have been subjected to evaporative concentration.

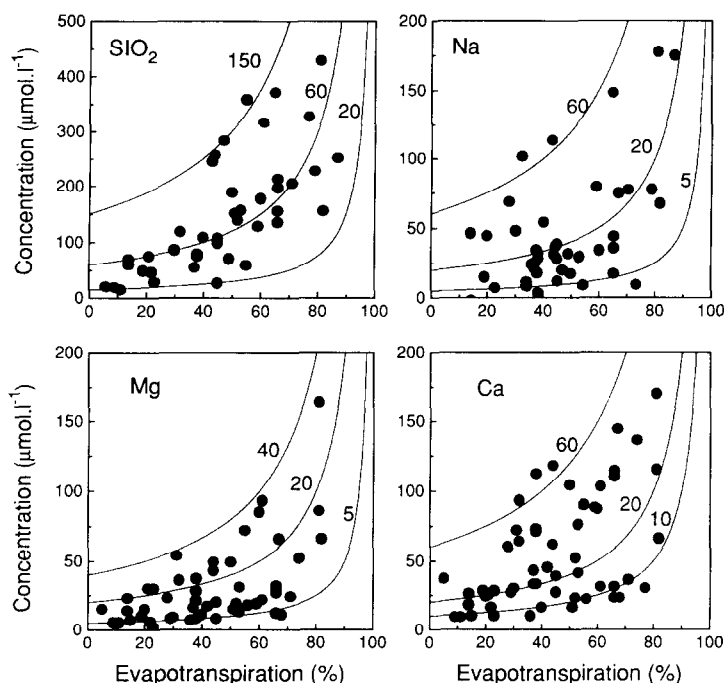


FIG. 4. Solute concentration vs. % water loss from ET. Lines denote evaporative trends from initial concentrations C_i^0 ($ET = 0$) as defined by Eqn. 11.

from 500 mm (Experimental Lake) to 4500 mm (Jamieson Creek). The proportions of input fluxes vary significantly between watersheds reflecting differences in geography (e.g., distance from the ocean), meteorology (e.g., direction and intensity of storm tracks), and the extent of interception by forest canopy. Watersheds with high precipitation (right side of Fig. 5) tend to have a low proportion of the total discharge flux contributed by chemical weathering. These watersheds

are close to the ocean, and have a large proportion of Na contributed by atmospheric deposition of sea salt. Therefore, the calculation of the Na weathering fluxes (Eqn. 5) in these watersheds is very susceptible to errors in the wet and dry deposition fluxes.

Mass balance calculations for Na produce negative fluxes for a number of watersheds (Fig. 5). Negative Na weathering fluxes (<0 on vertical axis) result when Na input fluxes from

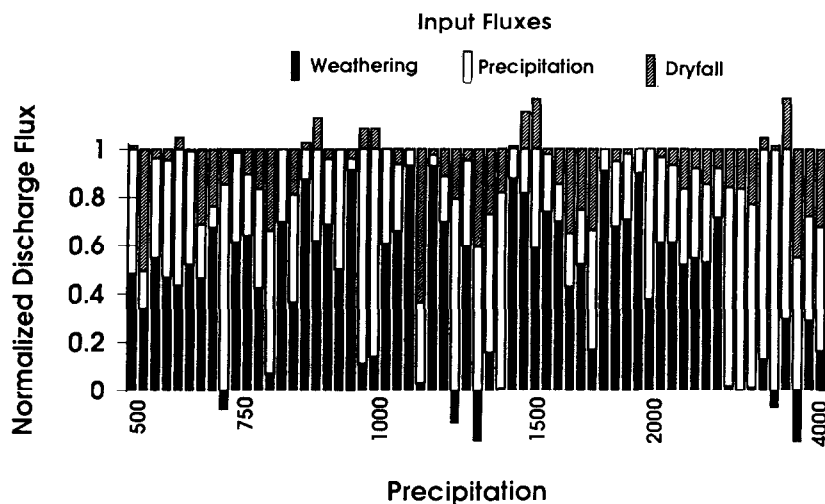


FIG. 5. Relative proportions of discharge flux (normalized to unity) contributed by chemical weathering, precipitation, and excess dryfall. Data bars for single watersheds are arranged (from left to right) in the order in increasing precipitation (from 600 to 4500 mm). Negative weathering fluxes (<0 on vertical axis) result from discharge fluxes being less than the sum of precipitation and excess dryfall (Eqn. 9). Negative dryfall (>1 on vertical axis) results from Cl discharge fluxes being less than inputs from precipitation (Eqn. 8). Such negative fluxes indicate errors in watershed budgets.

precipitation and dry fall exceed the discharge flux. Negative Na dryfall fluxes (>1 on vertical axis) reflect Cl balances in which the input from wet precipitation exceeds the discharge flux. Both conditions result from incorrect estimates of precipitation, runoff, or the presence of extraneous solute inputs from groundwater, road salts, and other sources. In the following climatic comparisons, watersheds with negative solute fluxes are excluded. Chemical species with lower concentrations in seawater tend to have lower proportions contributed by wet and dry precipitation (i.e., $\text{Na} > \text{K} > \text{Mg} > \text{Ca}$), and SiO_2 discharge fluxes are attributed solely to weathering. The ratio of input to weathering fluxes for other cations such as Ca and Mg show somewhat less variability than Na (Fig. 5), particularly in high precipitation watersheds.

SO_4 calculated as weathering fluxes can be either strongly positive or negative in individual watersheds. This high variability is attributed primarily to high (i.e., nonsteady-state) inputs of anthropogenic SO_4 in many watersheds, but also strong biogeochemical cycling, and significant volatility of S relative to the other elements. Charge balance constraints require that high outputs of SO_4 must be associated with an equivalence of cations. Such anomalous cation fluxes are deleted from climatic comparisons by excluding watersheds for which SO_4 discharge fluxes exceed precipitation fluxes by a factor of two (i.e., $Q_{\text{SO}_4, \text{dis}}/Q_{\text{SO}_4, \text{precip}} > 2$) when evaluating cation fluxes (but not SiO_2).

Weathering Fluxes vs. Precipitation

Watershed SiO_2 and Na fluxes increase with increasing precipitation and runoff (Fig. 6). The inserts in the figure 6 show more detail for the watersheds with SiO_2 fluxes $< 2000 \text{ mol} \cdot \text{ha}^{-1} \cdot \text{yr}^{-1}$ and Na fluxes $< 500 \text{ mol} \cdot \text{ha}^{-1} \cdot \text{yr}^{-1}$. The relationship between fluxes, precipitation (P), and runoff (R) can be approximated by the linear relationships

$$Q_i = a_0 + a_1 \cdot P \quad \text{and} \quad Q_i = a_0 + a_1 \cdot R, \quad (12)$$

Table 2. Linear regression parameters describing chemical fluxes in terms of precipitation and runoff (see Eqn. 6).

Flux (Q_i)	Intercept (a_0)	Slope (a_1)	N	r^2	P-value
precipitation					
SiO_2	211	0.380	44	0.51	<0.0001
Na	89	0.073	41	0.17	0.0040
Mg	54	0.034	60	0.13	0.0040
Ca	140	0.063	53	0.09	0.0252
K	28	0.006	53	0.04	0.1269
runoff					
SiO_2	409	0.360	44	0.42	<0.0001
Na	93	0.058	41	0.10	0.2040
Mg	82	0.020	57	0.05	0.0785
Ca	195	0.048	51	0.07	0.0744
K	33	0.006	50	0.04	0.1505

which are shown by the solid and dashed lines in Fig. 6. The slopes (a_0) and intercepts (a_1) and statistical parameters are shown in Table 2. The slopes of the SiO_2 trends (Fig. 6 insert) are nearly identical (0.38 and 0.36), as expected from the correspondence between precipitation and runoff shown in Fig. 2. Sodium fluxes exhibit poorer correlations than SiO_2 ($r^2 = 0.17$) reflecting difficulties in determining accurate Na and Cl balances in the high precipitation watersheds.

The full ranges for SiO_2 and Na weathering fluxes (right axes in Fig. 6) show that there are significant outliers to the datasets discussed above. The most obvious example is the tropical Rio Icacos rainforest site (22°C) which has a SiO_2 flux approximately five times greater than for the temperate rainforest watersheds of Jamieson Creek, British Columbia (4°C), and Indian River, Alaska (6°C). These differences occur despite similarities in annual precipitation, dense vegetation (although different species), very steep topography and high physical erosion rates in all these watersheds. High SiO_2 and Na fluxes also occur in the relatively warm Kiryu (13°C) and Tsukuba (14°C) watersheds of Japan compared to significantly lower fluxes from cooler watersheds with comparable precipitation (Fig. 6).

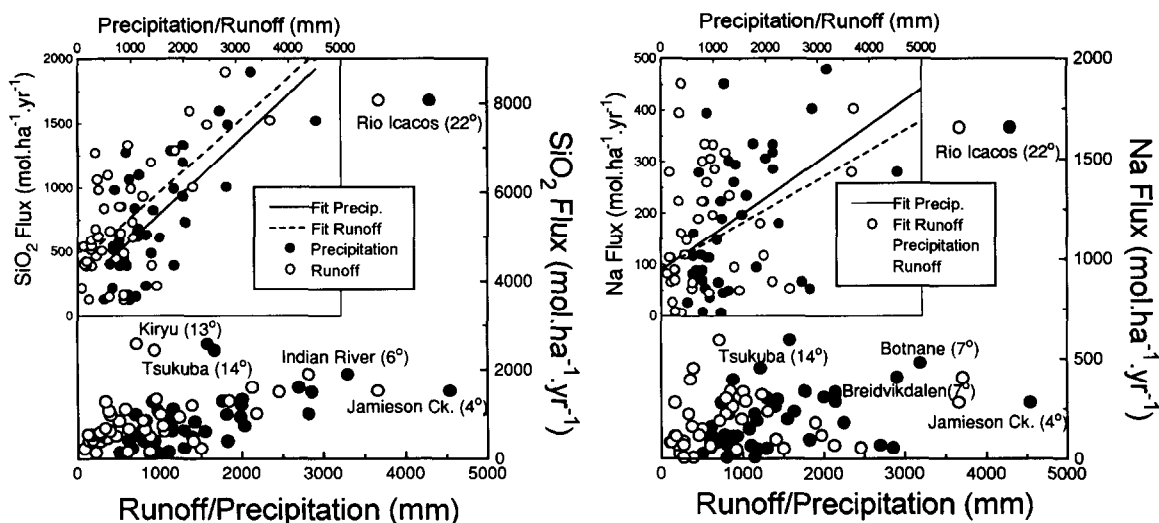


FIG. 6. Silica and Na weathering fluxes vs. precipitation (●) and runoff (○). The outer figures are inclusive of all data. Labels identify temperatures for outlier watersheds discussed in the text. The insert is an expanded view for watersheds with SiO_2 fluxes < 2000 and Na $< 500 \text{ mol/ha/yr}$. The solid and dashed lines correspond to the respective linear regression fits to precipitation and runoff (Eqn. 12) with parameters and statistics reported in Table 2.

Fluxes for Ca, Mg, and K showed minimal correlations with annual watershed precipitation and runoff (Table 2, $r^2 = 0.04\text{--}0.13$). Although weathering rates of minerals containing these cations are assumed to be influenced by differences in climate, discharge fluxes are more affected by differences in bedrock lithology, ion exchange, and biological cycling. Such variability between watersheds is apparently sufficient to obscure the effects of differences in precipitation.

Weathering Fluxes as Functions of Temperature

13 Effect of temperature on weathering rates (r) involving the dissolution of silicates is commonly described by an Arrhenius relationship

$$r_T = Ae^{(-E_a/RT)} \quad (13)$$

where E_a is the activation energy ($\text{kJ}\cdot\text{mol}^{-1}$), T is temperature ($^{\circ}\text{K}$), R is the gas constant, and A is a pre-exponential factor. The Arrhenius relationship (Eqn. 13) is derived for kinetics of simple well-characterized chemical reactions. Clearly, the application of Eqn. 13 to watershed solute fluxes involving multiple reactions and complex hydrochemical processes is not a rigorous approach. However, such an expression can be useful for empirically describing the dependence of weathering rates on temperature in natural systems. (Velbel, 1993a; Brady and Carroll, 1994).

The relationship between increasing SiO_2 and Na weathering fluxes and increasing temperature is shown in Fig. 7. The figure inserts show the linear relationship between logarithm of the weathering fluxes and the reciprocal of absolute temperature (Eqn. 13). The fit of Eqn. 13 to SiO_2 and Na data (solid lines) produce statistically meaningful regression coefficients (Table 3, $r^2 = 0.51$ and 0.48). The better correlation

14-15 Na fluxes with temperature (Fig. 7) compared to precipitation (Fig. 6) may result because the mass balance errors in high precipitation watersheds are less statistically significant.

Table 3. Arrhenius fit to temperature-dependent chemical fluxes (see Eqn. 13).

Flux mol/ha/yr	Preexp. A	E_a kJ	N	r^2	P-value
SiO_2	22	68.8	44	0.51	<0.0001
Na	39	78.2	43	0.48	<0.0001
Mg	9.8	12.4	60	0.00	0.5063
Ca	4.6	1.4	56	0.00	0.9420
K	22	42.7	53	0.07	0.0470

The respective activation energies for SiO_2 and Na (69 and $78 \text{ kJ}\cdot\text{mol}^{-1}$, Table 3) are also consistent with values commonly reported for experimental dissolution for silicates such as feldspars (e.g., Lasaga, 1984; Knauss and Wolery, 1986; Brantley et al., 1992). No obvious correlations were found between fluxes of Ca, Mg, and K and watershed temperature (Table 3) or precipitation and runoff (Table 2). Variations in weathering fluxes of these cations are related to processes not strongly correlated with climate.

The SiO_2 and Na fluxes plotted on outer linear scales in Fig. 7 demonstrate the exponential dependence of weathering rates on temperature (Eqn. 13). The solid lines show the same fit to the Arrhenius relationship as shown in the figure inserts, and significantly underestimate the SiO_2 and Na weathering rates of the Rio Icacos watershed which receives very high precipitation ($8060 \text{ mm}\cdot\text{yr}^{-1}$). High SiO_2 fluxes from the Kiryu and Tsukuba watersheds of Japan also correspond to high precipitation (1590 and 1670 mm). Lower SiO_2 fluxes from watersheds with comparable temperatures such as the Juliadale, Pond Branch, and Panola correspond to lower precipitation ($700\text{--}1150 \text{ mm}$). The influence of temperature on watershed weathering is apparently moderated by variations in precipitation.

DISCUSSION

The preceding results suggest that climatic conditions play a significant role in determining solute chemistry and weathering rates in watersheds.

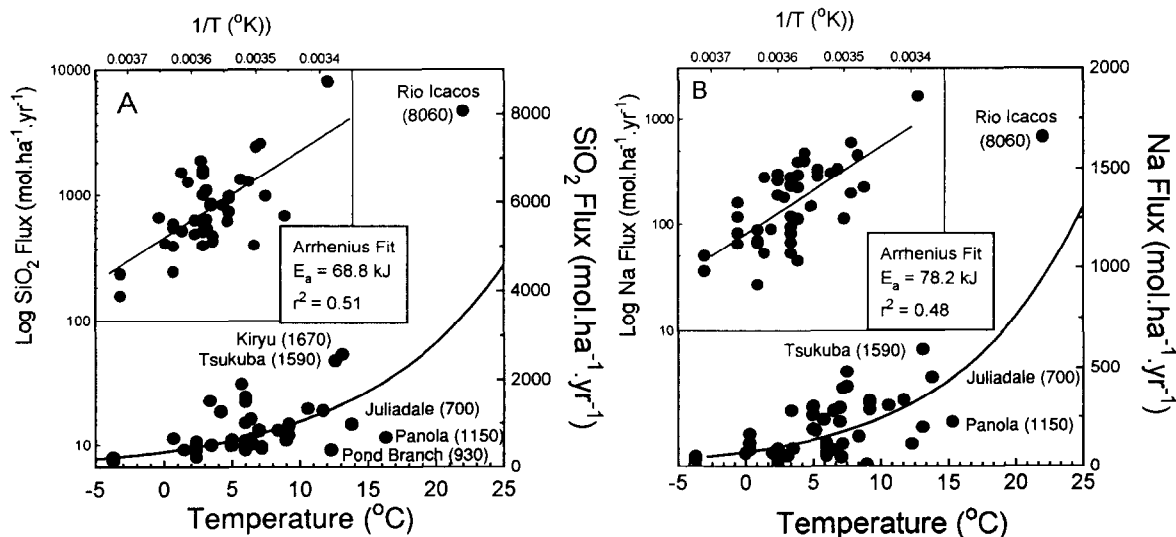


FIG. 7. Watershed SiO_2 and Na weathering fluxes vs. temperature ($^{\circ}\text{C}$). Inserts are Arrhenius plots of log fluxes vs. $1/T$. Diagonal lines correspond to linear regression fits to Eqn. 13 with activation energies and correlation coefficients indicated. Corresponding plots of data on linear scales are shown in the outer portions of the figures with indicated precipitation (mm) for selected watersheds.

Importance of *ET* and Climate in Determining Solute Concentration

The detailed hydrologic balances of the tabulated watersheds permit accurate assessments of annual *ET* (Table 1). *ET* accounts for up to ~90% of precipitation in several watersheds, and average *ET* for all the watersheds is 46%. The strong impact of *ET* in watershed hydrology, coupled with a correlation between *ET* and temperature, implies that mean solute discharge concentrations are not good indicators for differentiating weathering rates in watersheds with significantly different climates. For example, Meybeck (1986) presented concentration data for small river basins in France, many of which were underlain by granitic rocks. Silica concentrations decreased exponentially with increasing mean watershed elevation (100–2800 m), which corresponds to an estimated temperature range of 11 to –2°C. However, without corresponding hydrochemical budgets, it is ambiguous whether increased solute concentrations are the result of temperature-accelerated weathering or temperature-accelerated *ET*.

Calibrations for weathering feedback in global CO₂ models have relied principally on the solute chemistry of larger river basins compiled by Meybeck (1979, 1980). Although Meybeck's original work considered a matrix relating chemical fluxes and denudation rates to both temperature and runoff, subsequent climate models (Walker et al., 1981; Berner and Barron, 1984; Marshall et al., 1988; Brady, 1991; Brady and Carroll, 1994) have considered only the simplified effects of temperature on SiO₂ concentrations. Analysis of the present data, albeit on a smaller watershed scale, indicates that such solute concentrations are not accurate indicators of relative weathering intensities. Increasing trends in solute concentrations can result both from increases in weathering rates with temperature, as is assumed in the models, as well as from concentration effects produced by *ET*, which also increases with temperature. These dual climatic effects may explain the high apparent activation energies obtained from correlating temperature variations with river SiO₂ concentrations (e.g., 87 kJ·mol^{–1}; Marshall et al., 1988).

Variations in Cation Fluxes

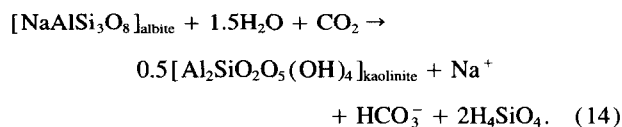
No statistical correlations are apparent between Ca, Mg, and K weathering fluxes and precipitation, runoff, or temperature (Tables 2, 3). Several earlier studies of regional watersheds and rivers have reported statistically significant linear or logarithmic increases in cation fluxes with runoff or temperature (Dunne, 1978; Peters, 1984; Meybeck, 1986; Dethier, 1986). These studies lacked the detailed hydrologic and chemical balances available for smaller watersheds. The absence of any correlation in the present study does not imply a lack of climatic impact on Ca, Mg, and K silicate weathering rates, only that these weathering fluxes are more dependent on other factors that exhibit greater variability between watersheds. This variability may be due to the presence of small amounts of sedimentary or hydrothermal calcites or dolomites present in some watersheds. Also, Ca, Mg, and K are major nutrients in biogeochemical cycles and the fluxes are influenced by the extent of degradation or aggradation of the veg-

etative cover. Finally, Ca, Mg, and K comprise the dominant exchangeable base cations in watershed soils and fluxes may be significantly affected by acid deposition. Weathering fluxes of Na are less susceptible to the above watershed processes. Sodium fluxes exhibit moderate statistical correlations with temperature (Fig. 7), but a poorer correlation with precipitation (Fig. 6), primarily because of the difficulty in determining Na weathering fluxes when marine aerosols and high precipitation cause large Na input fluxes.

Variations in Silica Fluxes

Relative to cations, SiO₂ fluxes exhibit stronger correlations with both temperature ($r^2 = 0.45$) and precipitation ($r^2 = 0.52$). Atmospheric inputs of silica are minimal, and therefore, less prone to measurement error. Silica is not a major biological nutrient, although there is some evidence for uptake, particularly for tropical soils (Lucas et al., 1993). Therefore, SiO₂ is not as susceptible as major cations to organic aggradation and degradation processes in watershed soils. Also, SiO₂ generally exists in watershed solutes as uncharged H₄SiO₄ that is less susceptible to soil ion exchange processes. Only circumstantial evidence exists for silica adsorption in soil environments (Casey and Neal, 1985).

Silica, however, is not a conservative solute. During weathering, SiO₂ is incorporated into secondary clays. Kaolinite is the most common weathering product of granitic rocks and the predominate clay mineral reported in the watershed studies. The weathering reaction for the albite component of feldspar, for example, can be represented as



The stoichiometry of the above reaction requires the aqueous release of two moles of SiO₂ for every mole incorporated with Al in the solid phases. If gibbsite forms in the watershed, three moles of SiO₂ will be released and if smectite forms, less SiO₂ will be mobilized (~1.4 moles for beidellite). The scatter in the SiO₂ fluxes is probably in part due to differences in secondary weathering products produced in different watersheds with different climates.

Annual Fluctuations in Watershed Fluxes

Weathering fluxes of SiO₂ and Na exhibit significant variations between watersheds that cannot be explained solely by differences in average precipitation and temperature. Some of the variability can be attributed to yearly variations in the climate of individual watersheds. Climate data are commonly reported on a yearly basis although monitoring at different sites varies from a single year to several decades. In the watershed tabulation (Table 1), average precipitation is established by summing all available annual values and dividing by the number of years of measurement.

SiO₂ fluxes in individual watersheds are strongly dependent on the annual precipitation for a specific year, which may vary by over a factor of two. In Fig. 8, annual SiO₂ fluxes are plotted against annual precipitation for several watersheds

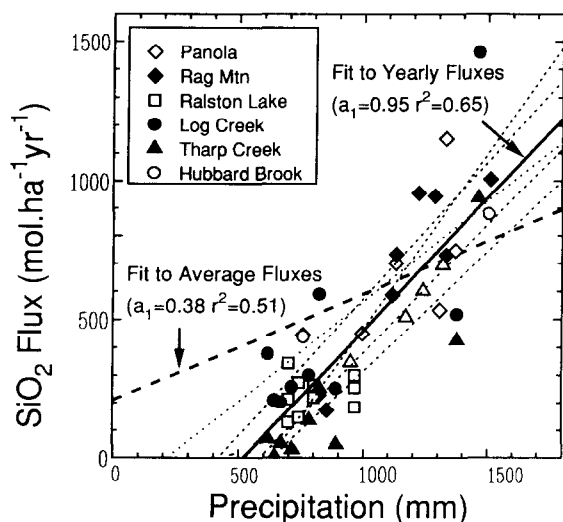


FIG. 8. Correspondence between SiO_2 fluxes and yearly precipitation for selected watersheds. Dotted lines are linear correlations for annual data for individual watersheds. Solid line is correlation to annual data for all watersheds. The dashed line represents the linear correlation established in Fig. 6 between average fluxes and precipitation for watersheds tabulated in Table 1.

with similar average precipitation (900–1300 mm, Table 1) and multiyear records. The slopes of the linear regression fits to individual watershed data range from 0.78 to 1.08 (not shown), while the slope of the fit to all the yearly data is 0.95 (solid line). A one-to-one correspondence between precipitation and SiO_2 fluxes (slope ≈ 1) results if solute concentrations in a watershed remain relatively constant with time, and the solute flux becomes directly proportional to the runoff or precipitation (Eqn. 4). This situation requires a significant reservoir of readily mobilized SiO_2 , most probably in soil porewaters or amorphous solids, which buffer the silica concentration during annual fluctuations in precipitation. This effect has been documented in long-term monitoring at sites such as at Hubbard Brook (Driscoll et al., 1989).

The SiO_2 fluxes of individual watersheds are more sensitive to yearly fluctuations in precipitation (slope = 1) than the variation in SiO_2 fluxes, with precipitation between watersheds based on averaged multiyear records (Table 1) shown by the dashed line in Fig. 8 (slope = 0.38, from Fig. 6). Over long time intervals, perhaps tens to hundreds of years, fluxes from individual watersheds must ultimately depend on the average weathering rates. However, short-term monitoring over one to several years can produce solute fluxes that are strongly dependent on transport-controlled processes and reflect annual precipitation trends. The comparison of SiO_2 fluxes and precipitation between watersheds more closely reflects the variations in the long-term weathering rate. However, annual variability undoubtedly accounts for a significant proportion of the scatter in fluxes in Table 1 and emphasizes the need for long-term watershed monitoring programs.

Reinforcement Effects of Precipitation and Temperature

Watersheds with extreme climatic conditions produce the most divergent weathering fluxes. This is illustrated by the much higher SiO_2 and Na weathering fluxes from the tropical

Rio Icacos rainforest, relative to the temperate rainforests with comparable precipitation in British Columbia and Alaska (Jamieson Creek and Indian River). Similar, but less dramatic differences are observed between other watersheds. Clearly, attempts to model weathering fluxes over climatic extremes based on the independent effects of precipitation and temperature is not satisfactory. In the present study, a function is proposed that quantitatively describes weathering fluxes of SiO_2 and Na as a coupled product of both precipitation and temperature

$$Q_{i,w} = (a_1 * P) \exp \left[-\frac{E_a}{R} \left(\frac{1}{T} - \frac{1}{T_0} \right) \right]. \quad (15)$$

The pre-exponential term on the right-hand side of Eqn. 15 assumes a linear correlation between precipitation and SiO_2 and Na fluxes where a_1 is the slope. The intercept a_0 is assumed to be zero (i.e., as precipitation approaches zero, weathering approaches zero). The form of this term is based on the approximate linear relationship between fluxes and precipitation shown in Fig. 6. The exponential temperature term in Eqn. 15 is equivalent to Eqn. 13, but describes the variation in fluxes as a function of the difference between T and a reference temperature T_0 (Brady, 1991). It must be recognized that no statistical correlation can unambiguously distinguish whether Eqn. 15 reflects the fundamental mechanisms of the weathering reaction. However, this coupled approach provides a more accurate empirical description of the variation in weathering fluxes than the individual consideration of precipitation and temperature.

Equation 15 can be solved numerically for the values of a_1 and E_a , which maximize the correlation between the predicted and measured watershed fluxes as functions of temperature and precipitation. Solutions to Eqn. 15 require the selection of a reference temperature (T_0), which was chosen to be 5°C , near the mean of the temperature data (Table 1). The solution for the activation energy (E_a) is insensitive to the choice of T_0 . In fitting Eqn. 15 to the watershed data, precipitation and temperature are treated as independent variables with respect to each other. In our dataset, the correlation between P and T has an $r^2 = 0.08$, suggesting that this is a valid assumption. The resulting fit of the SiO_2 data to the coupled precipitation-temperature function (Eqn. 15) produces values of $a_1 = 0.456$ and $E_a = 59.4 \text{ kJ} \cdot \text{mol}^{-1}$. The fit to the Na data produces slope and intercept values of $a_1 = 0.097$ and $E_a = 62.5 \text{ kJ} \cdot \text{mol}^{-1}$.

The correlation between the modeled and observed fluxes for SiO_2 and Na is shown in Fig. 9 and reflects the predictive capability of climate coupling (Eqn. 15). The high r^2 values (0.91 for SiO_2 and 0.83 for Na) are heavily controlled by the Rio Icacos watershed, although the lower flux watersheds also follow the model trends. For example, applying the same model to the SiO_2 data, excluding the Rio Icacos, yields values of $a_1 = 0.480$ and $E_a = 78.4 \text{ kJ} \cdot \text{mol}^{-1}$ with an $r^2 = 0.52$. Exclusion of the Rio Icacos site increases the uncertainty, and again illustrates the need for more watershed studies that span the extremes of temperature and precipitation.

The three-dimensional surface generated by Eqn. 15 and the fitted parameters for SiO_2 fluxes are shown in Fig. 10. A similar plot of Na fluxes has a nearly identical shape. The weathering flux varies linearly with precipitation along any constant temperature plane through the three-dimensional sur-

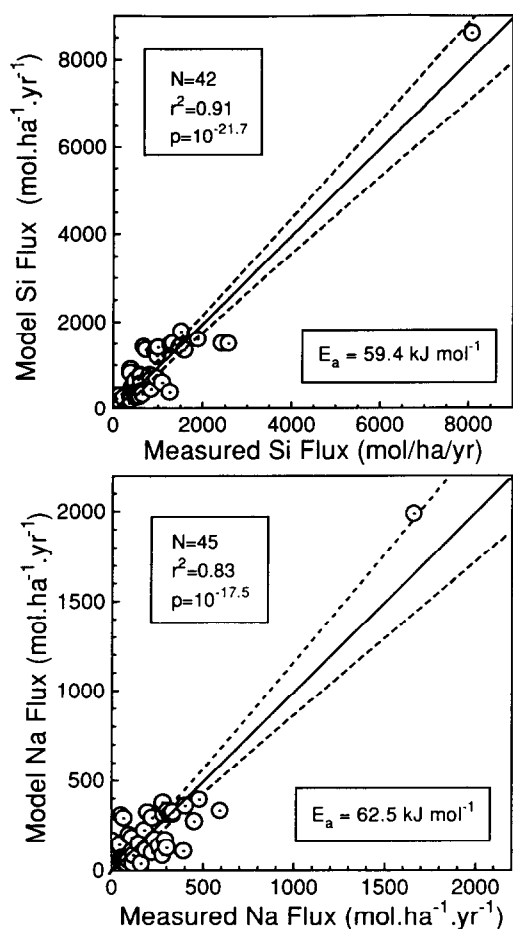


FIG. 9. Statistical correlation between measured and predicted SiO_2 and Na weathering fluxes based on the simultaneous consideration of temperature and precipitation (Eqn. 15). Also shown are the statistical parameters and calculated activation energies. Dashed lines represent 95% confidence bands.

face. However, the slope of the linear precipitation term increases exponentially with temperature. Therefore, the effect of precipitation is much greater in watersheds with higher temperatures than in watersheds with lower temperatures. Conversely, the weathering flux increases exponentially with temperature along any constant precipitation plane through the surface. However, the curvature of the temperature function is dependent on precipitation. For watersheds with low precipitation, the apparent exponential effect of temperature on weathering will be quite low. For wet watersheds, the exponential influence of temperature on weathering becomes very pronounced. The net effect of the above relationship is to reinforce weathering in watersheds with both high temperature and precipitation and to decrease weathering fluxes in watersheds with low temperature and precipitation.

Temperature-Corrected Fluxes

A useful way to evaluate the coupled effects of temperature and precipitation on watershed weathering is to correct the measured solute fluxes to constant values representative of average watershed conditions (5°C and 1000 mm precipita-

tion). This is equivalent to projecting the flux data onto planes parallel to the temperature and precipitation axes in Fig. 10. Temperature-corrected SiO_2 and Na fluxes (\circ) are plotted against precipitation in Fig. 11. Because the plot is generated at the reference temperature 5°C , the slope of the linear regression lines is equal to a_1 (Eqn. 15). When compared to the non-temperature compensated SiO_2 data (\bullet), the principal effect of the correction is to bring the higher temperature watershed fluxes in line with the lower temperature watersheds at comparable precipitation. This is most obvious for the tropical Rio Icacos watershed and the two relatively warm Japanese watersheds. The correlation between the corrected SiO_2 fluxes and precipitation now becomes $r^2 = 0.57$, a better fit than for the uncorrected data that excluded these high temperature sites ($r^2 = 0.51$; Fig. 6).

The temperature-corrected Na fluxes for the warmer watersheds also more closely approximate those of more temperate watersheds (Fig. 11). The statistical fit to the temperature-corrected Na flux data produced a correlation ($r^2 = 0.25$) that is significantly better than the poor correlation for the uncorrected data (Fig. 6, $r^2 = 0.10$). However, the coupling of temperature and precipitation effects for Na fluxes is only partially successful in overcoming errors caused by high atmospheric inputs of Na.

The preceding calculations correct all the watershed data to a reference temperature of 5°C . If another reference temperature is used, applicable for example to a regional watershed comparison, the slope (a_1) of an apparent precipitation vs. flux trend will change by a factor representing the Arrhenius temperature term. At 5, 10, 15, 20, and 25° , the temperature term will be 1.00, 1.57, 2.44, 3.72, and 5.60, and the corresponding slope of an apparent correlation between precipitation and flux will become 0.46, 0.72, 1.11, 1.70, and 2.55. These factors indicate the extent to which precipitation becomes increasingly effective in weathering as the temperature increases. Corresponding temperature correction factors expected for Na fluxes at 5, 10, 15, 20, and 25° are 1.000, 1.58, 2.46, 3.77, and 5.69, respectively.

Precipitation-Corrected Fluxes

SiO_2 and Na fluxes are corrected to a reference precipitation of 1000 mm in Fig. 12. The principal effect of the precipita-

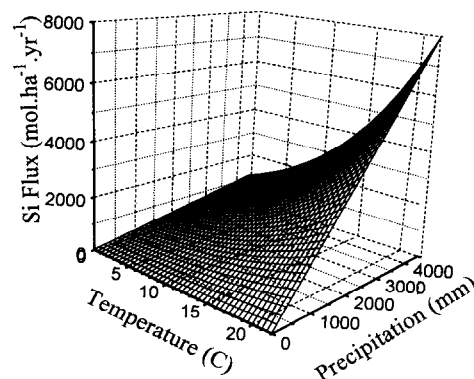


FIG. 10. Three-dimensional surface representing the optimized fit of watershed SiO_2 fluxes to Eqn. 15 as a function of precipitation and temperature.

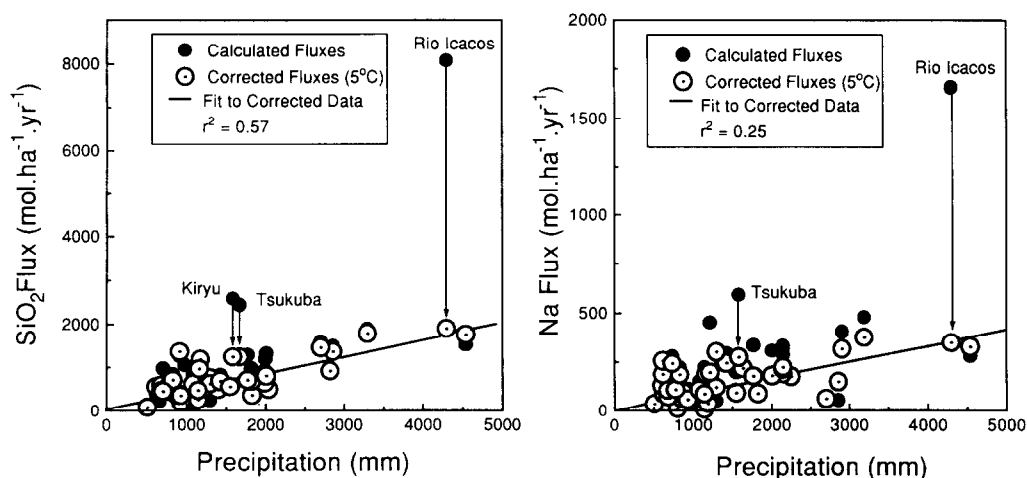


FIG. 11. Comparison of the precipitation dependence of uncorrected SiO_2 and Na fluxes (●) and fluxes normalized to 5°C (○) based on Eqn. 15. Solid lines are the linear regression fits to the temperature-corrected data. Arrows represent the extent of flux correction for selected high temperature/precipitation watersheds.

tion correction is to bring the weathering fluxes of SiO_2 and Na in the wetter watersheds (e.g., Rio Icacos, Kiryu, and Tsukuba) in line with the dryer watershed data. The curved lines in the figures represent the optimization fit of Eqn. 15. The curvatures of the temperature trends are considerably less than those generated by the optimization of the uncorrected temperature data (Fig. 7), reflecting lower activation energies. The precipitation-corrected SiO_2 and Na fluxes plotted in the Arrhenius format (Fig. 12 inserts) produce generally linear distributions. The activation energies for SiO_2 of 59.4 kJ and for Na of 62.5 kJ are significantly lower than for the uncorrected data (Table 3, SiO_2 = 68.8 kJ, Na = 78.2 kJ). The optimization of Eqn. 15, and therefore the calculated activation energies, are strongly dependent on a limited number of

high temperature watersheds. This is illustrated by the optimization passing very near the Rio Icacos data point (Fig. 12, solid lines).

Mechanisms of Chemical Weathering

The calculated SiO_2 and Na activation energies are very similar (59.4 and 62.5 $\text{kJ} \cdot \text{mol}^{-1}$), while the sources of uncertainty for the SiO_2 and Na fluxes are quite different. As discussed earlier, SiO_2 is not conservative during weathering and the SiO_2 flux out of a watershed is dependent on both the stoichiometry of the minerals weathering and the secondary clays that precipitate. However, SiO_2 input fluxes to watersheds are negligible, and a small source of error. In contrast,

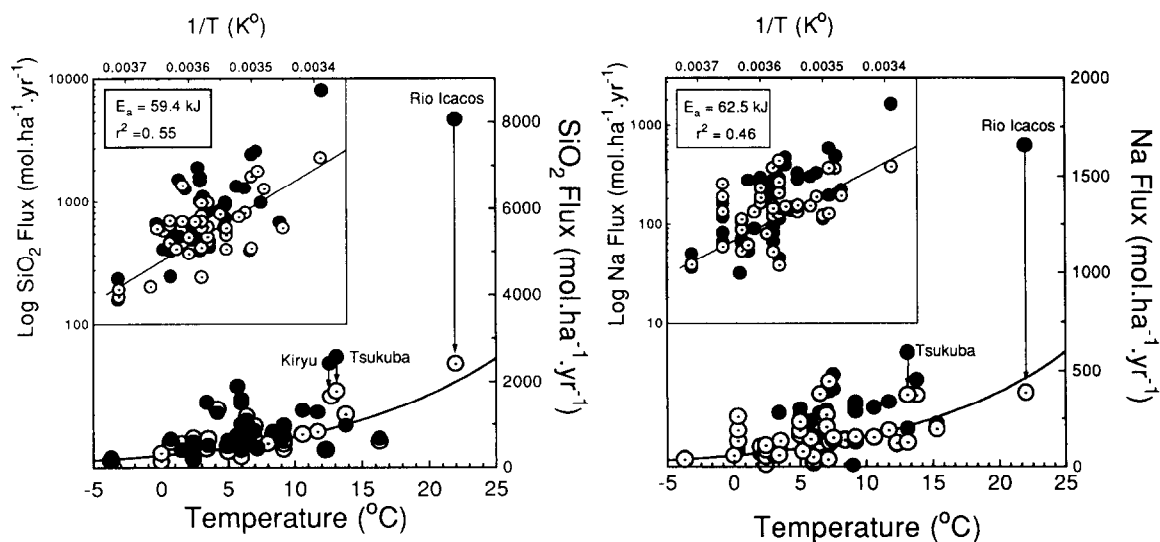


FIG. 12. Comparison of the temperature dependence ($^{\circ}\text{C}$) of uncorrected SiO_2 and Na fluxes (●) and fluxes normalized to 1000 mm of precipitation (○) based on Eqn. 15. Inserts are Arrhenius plots of log fluxes vs. $1/T$. Solid lines are the regression fits to the temperature-corrected data with slopes proportional to indicated activation energies. Arrows represent the extent of flux correction for selected high temperature/precipitation watersheds.

Na is nearly conservative during weathering and the major error in Na budgets is the input flux. The differences in potential errors in the flux data, and the very different chemical behavior of SiO_2 and Na, strongly suggest that the similarities in calculated activation energies are the result of a similar underlying weathering process, and not the result of some other unrecognized biogeochemical process.

SiO_2 and Na activation energies also fall within the range of values determined from experimental feldspar dissolution. Knauss and Wolery (1986) and Brantley et al. (1992) suggested values of 55 and 60 $\text{kJ} \cdot \text{mol}^{-1}$ for albite, respectively. Sverdrup (1990) reports activation energies of 64 and 80 $\text{kJ} \cdot \text{mol}^{-1}$ for albite and oligoclase, respectively. In the only previous study using watershed data, Velbel (1993a) obtained an activation energy of 77 $\text{kJ} \cdot \text{mol}^{-1}$ for Na fluxes based on a temperature difference of 1.1°C between the Coweeta 2 and 34 watersheds (Table 1).

In Eqn. 15, the impact of the activation energy on chemical fluxes is modified by a pre-exponential term, which is linearly proportional to precipitation. This dependence implies that increasing precipitation and moisture become progressively more important in weathering reactions at higher temperatures. Water content has long been considered an important parameter in weathering and soil development (Ollier, 1984), but has only recently been considered in terms of weathering mechanisms (Brantley et al., 1992; Velbel, 1993b). Increasing precipitation, moisture, and solvent throughput can effect the unsaturated hydrology of the soil zone and accelerate weathering rates by increasing the wetted reactive surface areas of minerals. In addition, as soils become wetter, stagnant porewaters that are immobile under drier conditions become hydrologically connected and potentially active weathering sites.

Besides physical and hydrological aspects, increased precipitation and moisture may decrease soil solution concentrations and decrease soil pH. Burch et al. (1993) experimentally observed a strong dependence of albite dissolution on reaction affinity as solutions approach thermodynamic equilibrium. Presumably, concentrated soil solutions in watersheds with low precipitation (Fig. 3) would be thermodynamically closer to equilibrium than in wetter watersheds and may exhibit slower weathering rates. High solute concentrations may also promote the inhibitory effects of Al and other species that have been experimentally shown to inhibit feldspar dissolution (Amrhein and Suarez, 1992; Olkers et al., 1994). Solutions at low pHs (<4) have been shown experimentally to strongly accelerate feldspar dissolution (summary, see Blum, 1994). The stream pHs in the tabulated watersheds (Table 1) range from 4.6 to 6.9 (Table 1) and exhibit no correlation with SiO_2 and Na fluxes. However, the pH in soil waters may be significantly lower than the streams because of higher organic acids and soil P_{CO_2} in the soil solution, and this may influence weathering reactions. Some combination of these hydrologic and chemical effects are probably responsible for the correlation between the SiO_2 fluxes and annual precipitation of individual watersheds (Fig. 6).

Chemical vs. Physical Weathering

Physical erosion is an additional factor that can potentially contribute to significant differences in chemical weathering

fluxes in watersheds. As discussed above, much ongoing weathering does not involve fresh bedrock but occurs in the soil zone. Soils have significantly different mineralogy than bedrock, due to long-term selective weathering. Stallard and Edmond (1983) differentiated such mineral selectivity in terms of weathering-limited and transport-limited regimes. In a weathering-limited regime, mechanical erosion is faster than chemical weathering. Therefore, the most reactive phases will always be available for weathering. For example, calcite dissolution dominates Ca and alkalinity fluxes in the alpine Loch Vale watershed (Table 1), which has been impacted by recent glaciation (Mast et al., 1990). This occurs even though hydrothermal calcite is present in only trace amounts in the igneous and high grade metamorphic rocks. In a transport-limited regime, physical erosion is less intense and weathering is less selective. All weatherable minerals ultimately contribute to the solute load in proportion to their abundances in the bedrock. This is the case for nearly complete weathering of primary aluminosilicates from the Rio Icacos soils (Blum et al., 1993).

Sediment transport, the most direct method for measuring physical erosion in watersheds, is not reported for the majority of the watersheds considered. However, as discussed by Berner and Berner (1987), average topography or steepness may be a qualitative indicator of the degree of physical erosion, particularly for similar rock types. The average watershed slopes were estimated by dividing the elevation gain (maximum minus minimum elevations, Table 1) by the length of the watershed axis, calculated by assuming the watershed is an isosceles triangle with an apex of 30°. The calculation produced slopes that varied between 0.01 and 0.45 m/m (Fig. 13). Topographic relief is required to hydrologically define a research watershed, and therefore, flat topographies are not represented. For the land surfaces considered, no correlation exists between slope and SiO_2 and Na weathering fluxes (Fig. 13). Therefore, implied physical erosion rates do not appear to be a dominant impact on chemical weathering rates.

Consequence studies show a significant decrease in the chemical weathering rates of soils over time due to the pref-

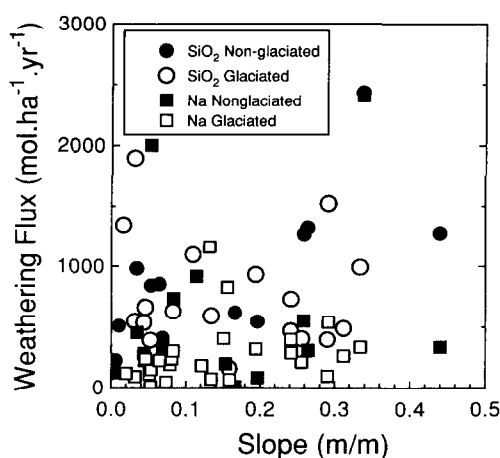


FIG. 13. SiO_2 and Na weathering flux vs. hill slope steepness calculated from elevation and watershed areas tabulated in Table 1. Data are differentiated as to the occurrence or absence of glaciation in the last 8–12 ka years.

removal of reactive minerals (White et al., 1992, 1994). Therefore, watersheds with younger soils and a significant percentage of exposed bedrock may be expected to have higher weathering rates. This hypothesis can be tested by comparing weathering fluxes for glaciated and nonglaciated watersheds. The flux data plotted in Fig. 13 were differentiated by whether the watershed was glaciated in the last 8–10 ka. For watersheds for which no Pleistocene geological records are available, estimates were made from the areal extent of continental glaciation. Figure 13 shows no clear differentiation of SiO_2 and Na fluxes from watersheds that have experienced recent alpine glaciation (e.g., Loch Vale, Emerald Lake, Log Creek), those that experienced Pleistocene glaciation (e.g., Hubbard Brook, Bear Brook, and Rawson Lake), and those which have not been glaciated in at least 250 ka (e.g., Panola, Brair Creek, and Rusape). This implies that past glaciation does not greatly affect present chemical weathering rates in these watersheds. The preceding data suggest that the effects of watershed topography, physical erosion rates, and soil ages are of secondary importance relative to precipitation and temperature in controlling weathering rates.

Watershed vs. River Fluxes

Watershed SiO_2 and Na weathering fluxes (Table 1) can be compared to world river fluxes calculated from average chemical concentrations and basin runoffs reported by Berner and Berner (1987). The areal extent of these river basins are two to six orders of magnitude greater and contain heterogeneous lithologies, so that the net fluxes usually involve weathering of nonsilicates. However, the overall distribution of watershed SiO_2 fluxes is only slightly higher than river fluxes, and the average SiO_2 fluxes are similar ($1040 \text{ mol} \cdot \text{ha}^{-1} \cdot \text{y}^{-1}$ vs. $960 \text{ mol} \cdot \text{ha}^{-1} \cdot \text{y}^{-1}$). The distributions of Na fluxes in the watersheds and rivers are nearly identical as are the average fluxes (414 vs. $360 \text{ mol} \cdot \text{ha}^{-1} \cdot \text{y}^{-1}$). These similarities are surprising, considering that watersheds are upland headwaters of large river systems and are commonly typified as having anomalously high rates of both physical and chemical weathering (Stallard and Edmond, 1983). Similarities in fluxes suggest either that the topographically flat regions of river basins have higher rates of chemical weathering than previously assumed, or else the chemical weathering of granitic rock types is much slower than for upland watersheds with other rock types.

Application to Climate Models

A number of climate models have considered the mechanism that stabilizes global climate over geologic time due to the feedback between atmospheric CO_2 and silicate weathering (Walker et al., 1981; Berner et al., 1983; Volk, 1987; Marshall et al., 1988; Brady, 1991; Berner, 1994). The major uncertainty in such models is the sensitivity of weathering rates to climatic variables, principally temperature, precipitation, and runoff.

The effect of climate on weathering rates can be expressed as the ratio of the weathering rate to that at a reference climate (r_0), in this case, 5°C and 1000 mm of precipitation (r/r_0 in Fig. 14, as defined by Brady, 1991). Figure 14 shows the

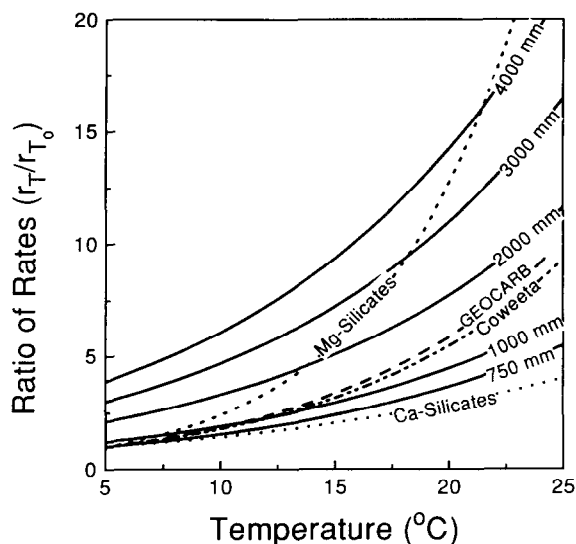


FIG. 14. Ratios of rates of SiO_2 weathering as functions of temperature at constant precipitation predicted by this study (solid lines). Standard state (r_0) is 5°C and 1000 mm of precipitation. Dotted lines are rate ratios based on experimental activation energies for Mg and Ca silicates (Brady and Carroll, 1994). Dash-dotted line is based on activation energies established from solute fluxes at the Coweeta watershed (Velbel, 1993a). Dashed line is trend predicted by the GEOCARB II model (Berner, 1994).

predictions of Eqn. 15 for constant precipitation from 300–4000 mm. These results, except at high precipitation and low temperature, are bracketed by the Arrhenius relationships based on the experimental activation energies proposed by Brady (1991) for Ca silicates ($48 \text{ kJ} \cdot \text{mol}^{-1}$) and Mg silicates ($115 \text{ kJ} \cdot \text{mol}^{-1}$). The calculated activation energies based on watershed SiO_2 and Na fluxes (59 and $62 \text{ kJ} \cdot \text{mol}^{-1}$) fall between these experimental values. Also included in Fig. 14 is the predicted temperature dependence based on the activation energy of $77 \text{ kJ} \cdot \text{mol}^{-1}$ obtained by Velbel (1993a) from the Coweeta watersheds.

Recently, Berner (1994) in the GEOCARB II model considered the coupled effects of temperature and runoff on apparent weathering fluxes. This model was calibrated using an activation energy of $62 \text{ kJ} \cdot \text{mol}^{-1}$ (Brady, 1991) and river runoff/concentration data presented by Dunne (1978) and Peters (1984). Observed trends in solute concentrations were assumed to result from the combined effects of dilution (i.e., Eqn. 2) and solute residence times in the regolith. As in previous models, the effects of ET on solute concentrations were not considered. This model also assumes that the reaction rates are not kinetically influenced by moisture content as is suggested in the present study. Figure 14 indicates that weathering rates produced by GEOCARB II and the present coupled approach (Eqn. 15) produce comparable rates for moderate precipitation environments (1000 – 2000 mm) but that the GEOCARB II weathering would significantly underestimate watershed weathering rates in wet tropical environments.

The weathering model presented in this study suggests that weathering rates are accelerated in wet, warm climates, and a larger proportion of global weathering will occur in tropical

23 regions. This has three major implications for global weathering/climatic models. First, global silicate weathering through geologic time should be very sensitive to the area of landmass in the tropical latitudes, as suggested by Worsley and Kidder (1991). Secondly, because the major changes in climate during global warming are in the temperate and Arctic regions, areas which contribute a disproportionately small amount of global weathering, the feedback between climate and weathering rates should be weaker using this model than using weathering rates calculated using average continental temperatures and precipitation. Finally, this study indicates there is not a strong relationship between steep topography and high chemical weathering rates, and therefore, does not lend support to the concept of tectonic control of global climate (e.g., Raymo, 1991; Raymo and Ruddiman, 1992; Edmond, 1992).

CONCLUSIONS

This study examined the impact of precipitation, runoff, and temperature on chemical concentrations and fluxes from experimental watersheds underlain by granitoid rocks. In watersheds with similar temperatures, the amount of *ET* is fairly constant and independent of precipitation and runoff. However, the proportion of precipitation lost by *ET* increases with lower precipitation, and this results in evaporation concentration of major cations in watershed streams. 24 ion concentrations are, therefore, not an effective method for comparing weathering rates between watersheds with widely different climates.

25 Watershed solute fluxes are not susceptible to *ET* effects, and weathering fluxes of SiO_2 and Na are employed to quantify the effects of precipitation and temperature on weathering rates. Fluxes of Ca, Mg, and K must also reflect significant weathering input, but climatic variability is obscured by other differences between watersheds, such as lithology, nutrient cycling, and ion exchange. Attempts to describe SiO_2 and Na fluxes as an independent linear function of precipitation and exponential (Arrhenius) function of temperature produced statistically meaningful correlations, but also demonstrated consistent anomalies, particularly for watersheds with wet and warm climates.

26 This variability led to the development of a function for describing the dependence of weathering rates on climate which is the product of a linear effect of precipitation and an Arrhenius temperature dependence. This function produces a linear correlation between precipitation and weathering rates at any fixed temperature, but the slope of the precipitation correlation increases exponentially with increasing temperature. This results in accelerated weathering rates in watersheds with both high precipitation and warm temperatures, and decreased weathering rates in watersheds with either low temperature or precipitation. The activation energies calculated from this model are compatible with weathering rates dominated by silicate mineral dissolution. This model which couples the effects of precipitation and temperature provides an improved description of silicate weathering rates in watersheds spanning a wide range of climatic regimes. There are no obvious trends between weathering fluxes and watershed slope steepness or recent glaciation, suggesting that topogra-

phy and physical erosion are less important than temperature and precipitation in controlling chemical weathering rates in watersheds.

This study indicates that the effects of precipitation and temperature must be considered simultaneously when modeling the feedback between climate and chemical weathering rates. Comparison with previous models indicates comparable results for temperate climatic conditions, but the present study more accurately describes the effects of precipitation and temperature under greater extremes of climatic conditions. The nonlinear nature of the proposed feedback between climate and weathering, with an enhanced importance of tropical regions, suggests that global models based on changes in average continental temperature and precipitation do not adequately represent the effects of global climatic change on chemical weathering rates.

Acknowledgments—The authors acknowledge a significant number of individuals who contributed additional unpublished data to the watershed tabulation, including Gary Buell, Owen Bricker, George H. Leavesley, Norman E. Peters, and Michael M. Reddy of the US Geological Survey, J. P. Kimmins of the University of British Columbia, Emergy T. Cleaves of the Maryland Geological Survey, Richard F. Yuretich of the University of Massachusetts, Paul P. Campbell of the Canadian Fresh Water Institute, Steve Norton of the University of Maine, Tony Edwards of the Macaulay Land Use Institute, Dan Everson of the US National Park Service, Martin Forsius and Sirpa Kleemola of the Finnish Water and Environmental Institute, Tatemasa Hirata of the Japanese National Institute for Environmental Studies, Espen Lydersen of the Noesk Institutt for Vannforskning, and Ulla Maria Calles of the Swedish National Power Board. The paper also benefited from reviews by Owen Bricker, James Shanley, and Michael Velbel.

Editorial handling: T. Pačes

REFERENCES

- Allen C. J., Roulet N. T., and Hill A. R. (1993) The biogeochemistry of pristine headwater Precambrian shield watersheds: an analysis of material transport within a heterogeneous landscape. *Biogeochemistry* **22**, 37–79.
- Amiotte-Suchet P. A. and Probst J. L. (1993) Modelling of atmospheric CO_2 consumption by chemical weathering of rocks: Application to the Garonne, Congo and Amazon basins. *Chem. Geol.* **107**, 205–210.
- Amrhein C. and Suarez D. L. (1992) Some factors affecting the dissolution kinetics of anorthite at 25°C. *Geochim. Cosmochim. Acta* **56**, 1815–1826.
- April R., Newton R., and Coles L. T. (1986) Chemical weathering in two Adirondack watersheds: Past and present rates. *Geol. Soc. Amer.* **97**, 1232–1238.
- Avila A. and Rodà F. (1988) Export of dissolved elements in an evergreen-oak forest in the Montseny Mountains (SE Spain). *Catena Supplement* **12**, 1–12.
- Bergström L. and Gustafson A. (1985) Hydrogen ion budgets of four small runoff basins in Sweden. *Ambio* **14**, 346–349.
- Berner R. A. (1991) Model for atmospheric CO_2 over Phanerozoic time. *Amer. J. Sci.* **291**, 339–376.
- Berner R. A. (1992) Weathering, plants, and the long term carbon cycle. *Geochim. Cosmochim. Acta* **56**, 3225–3231.
- Berner R. A. (1994) GEOCARB II: A revised model of atmospheric CO_2 over Phanerozoic time. *Amer. J. Sci.* **294**, 56–91.
- Berner R. A. and Barron E. J. (1984) Comments on the BLAG model: Factors affecting atmospheric CO_2 and temperature over the past 100 million years. *Amer. J. Sci.* **284**, 1183–1192.
- Berner E. K. and Berner R. A. (1987) *The Global Water Cycle: Geochemistry and the Environment*. Prentice-Hall.

- Berner R. A., Lasaga A. C., and Garrels R. M. (1983) The carbonate-silica geochemical cycle and its effect on atmospheric carbon dioxide and climate. *Amer. J. Sci.* **283**, 641–683.
- Blum A. E. (1994) Feldspars in weathering. In *Feldspars and Their Reactions* (ed. I. Parsons); NATO Advanced Study Workshop, Series C, pp. 595–629. Kluwer.
- Blum A. E., White A. F., Bullen T., Schulz M. S., and Larson M. (1993) Chemical weathering of silicate minerals in a mountainous tropical rain forest, Puerto Rico. *GSA Abstr. Annu. Mtg.*, A-255 (abstr.).
- Bouchard M. (1983) Bilan géochimique et origine d'éléments dissous dans un bassin-versant granitique breton (France). *Revue Géol. Dynam. Géogr. Phys.* **24**, 363–379.
- Brady P. V. (1991) The effect of silicate weathering on global temperature and atmospheric CO₂. *J. Geophys. Res.* **96**, 18 101–18 106.
- Brady P. V. and Carroll S. A. (1994) Direct effects of CO₂ and T on silicate weathering: Possible implications for climate control. *Geochim. Cosmochim. Acta* **58**, 1853–1856.
- Brantley S. L., Stillings L. L., and Voigt D. E. (1992) Effect of oxalic acid on albite dissolution. *Abstr. Papers, 203rd ACS Natl. Mtg. GEOC 4*, 239.
- Bricker O. P. and Rice K. (1989) Acidic deposition to streams. *Environ. Sci. Technol.* **23**, 379–385.
- Bruijnzeel L. A. (1990) *Hydrology of Moist Tropical Forests and Effects of Conversion: A State of Knowledge Review*. UNESCO Intl. Hydrol. Programme, Free Univ. Amsterdam.
- Buell G. R. and Peters N. E. (1988) Atmospheric deposition effects on the chemistry of a stream in northwest Georgia. *Water Air Soil Pollut.* **25**, 125–135.
- Burch T. E., Nagy K. L., and Lasaga A. C. (1993) Free energy dependence of albite dissolution kinetics at 80°C and pH 8.8. *Chem. Geol.* **105**, 137–162.
- Calles U. M. (1983) Dissolved inorganic substances. *Hydrobiologia* **101**, 13–18.
- Casey H. and Neal C. (1985) Abiological controls on silica in chalk streams and groundwater. In *Sediments and Water Interactions* (ed. P. G. Sly), pp. 332–334. Springer-Verlag.
- Clayton J. L. (1986) An estimate of plagioclase weathering in the Idaho Batholith based upon geochemical transport rates. In *Rates of Chemical Weathering* (ed. S. M. Coleman and D. P. Dethier), pp. 453–466. Academic.
- Cleaves A. T., Godfrey A. E., and Bricker O. P. (1970) Geochemical balance in a small watershed. *GSA Bull.* **81**, 3013–3032.
- Cooper D. M., Morris E. M., and Smith C. J. (1987) Precipitation and streamwater chemistry in a subarctic Scottish catchment. *J. Hydrol.* **93**, 221–240.
- Creasey J., Edwards A. C., Reid J. M., Macleod D. A., and Cresser M. S. (1986) The use of catchment studies for assessing chemical weathering rates in two contrasting upland areas of Northeast Scotland. In *Rates of Chemical Weathering of Rocks and Minerals* (ed. S. M. Colman and D. P. Dethier), pp. 467–501. Academic.
- Cresser M. and Edwards A. (1987) *Acidification of Freshwaters*. Cambridge Univ. Press.
- Dethier D. P. (1986) Weathering rates and chemical fluxes from catchments in the Pacific Northwest U.S.A. In *Rates of Chemical Weathering of Rocks and Minerals* (ed. S. M. Colman and D. P. Dethier), pp. 503–528. Academic.
- Drever J. L. and Zobrist J. (1992) Chemical weathering of silicate rocks as a function of elevation in the southern Swiss Alps. *Geochim. Cosmochim. Acta* **56**, 3209–3216.
- Driscoll C. T., Likens G. E., Hedlin L. O., Eaton J. S., and Borman F. H. (1989) Changes in the chemistry of surface waters. *Environ. Sci. Technol.* **23**, 137–142.
- Dunne T. (1978) Rates of chemical denudation of silicate rocks in tropical catchments. *Nature* **274**, 244–246.
- Farley D. A. and Werritty A. (1989) Hydrologic budgets for the Loch Dee experimental catchments, Southwest Scotland (1981–1985). *J. Hydrol.* **109**, 351–368.
- Fever K. H., Brahmer G., and Zöttl H. W. (1990) Element budgets of two contrasting catchments in the Black Forest (Federal Republic of Germany). *J. Hydrol.* **116**, 85–99.
- Feller M. C. and Kimmins J. P. (1984) Effects of clearcutting and slash burning on streamwater and watershed nutrient budgets in southwestern British Columbia. *Water Res. Res.* **45**, 1421–1437.
- Frogner T. (1990) The effect of acid deposition on cation fluxes in artificially acidified catchments in western Norway. *Geochim. Cosmochim. Acta* **54**, 769–780.
- Garrels R. M. and Mackenzie F. T. (1971) *Evolution of Sedimentary Rocks*. W. W. Norton Inc.
- Hirata T. and Muraoka K. (1993) The relationship between water migration and chemical processes in a forest ecosystem. In *Tracers in Hydrology; IAHS Publ.* **215**, pp. 31–55.
- Johnson N. M., Likens G. E., Borman F. H., Fisher D. W., and Pierce R. S. (1969) A working model for the variation in stream chemistry at the Hubbard Brook Experimental Forest, New Hampshire. *Water Res. Res.* **5**, 1353–1363.
- Knauss K. G. and Wolery T. J. (1986) Dependence of albite dissolution kinetics on pH and time at 25°C and 70°C. *Geochim. Cosmochim. Acta* **50**, 2481–2497.
- Krauskopf K. B. (1967) *Introduction to Geochemistry*. McGraw-Hill.
- Lasaga A. C. (1984) Chemical Kinetics of Water-Rock Interactions. *J. Geophys. Res.* **89**, 4009–4025.
- Lewis W. M., Jr. and Grant M. C. (1979) Changes in the output of ions from a watershed as a result of the acidification of precipitation. *Ecology* **60**, 1093–1097.
- Lepisto A., Whitehead P. G., Neal C., and Cosby B. J. (1988) Modeling the effects of acid deposition: Estimation of long term water quality responses in forested catchments in Finland. *Nordic Hydrol.* **19**, 99–120.
- Likens G. E., Bormann F. H., Pierce R. S., Eaton J. S., and Johnson N. M. (1977) *Biogeochemistry of a Forested Ecosystem*. Springer Verlag.
- Lucas Y., Luiza F. J., Chauvel A., Rouiller J., and Nahon D. (1993) The relationship between biological activity of the rain forest and mineral composition of soils. *Science* **260**, 521–523.
- Marchard D. E. (1971) Rates and modes of denudation, White Mountains, Eastern California. *Amer. J. Sci.* **270**, 109–135.
- Marshall H. G., Walker J. C. G., and Kuhn W. R. (1988) Long-term climate change and the geochemical cycle of carbon. *J. Geophys. Res.* **93**, 791–801.
- Mast M. A., Drever J. I., and Baron J. (1990) Chemical weathering in Loch Vale Watershed, Rocky Mountain National Park, Colorado. *Water Res. Res.* **26**, 2971–2978.
- McDowell W. H. and Asbury C. E. (1994) Export of carbon, nitrogen, and major ions from three tropical montane watersheds. *Limnol. Oceanogr.* **39**, 111–125.
- Meybeck M. (1979) Concentration des eaux fluviales en éléments majeurs et apports en solution aux océans. *Rev. Géol. Dynam. Géogr. Phys.* **21**, 215–246.
- Meybeck M. (1980) Pathways of major elements from land to oceans through rivers. In *Inputs to Ocean Systems* (ed. J. M. Martin et al.); UNEP, IOC, SCOR Workshop Proc., pp. 18–30.
- Meybeck M. (1986) Composition chimique des ruisseaux non pollués de France. *Sci. Géol. Bull.* **39**, 3–77.
- Norton S. A. et al. (1994) Response of the West Bear Brook Watershed, Maine to the addition of (NH₄)₂SO₄—Three year results. *Forest Ecol. Manage.* **68**, 61–73.
- Ogden J. G. (1980) Comparative composition of continental and Nova Scotian precipitation. *Proc. Intl. Conf. Ecol. Impact Acid Precip. SNSF Proj.*, Oslo, pp. 125–130.
- Olkers E. H., Schott J., and Devidal J. L. (1994) The effect of aluminum, pH, and chemical affinity on the rates of aluminosilicate dissolution reactions. *Geochim. Cosmochim. Acta* **58**, 2011–2024.
- Ollier C. (1984) *Weathering*. Longman.
- Owens L. B. and Watson J. P. (1979) Rates of weathering and soil formation on granite in Rhodesia. *Soil Sci. Soc. Amer. J.* **43**, 160–166.
- Pačes T. (1985) Sources of acidification in Central Europe estimated from elemental budgets in small basins. *Nature* **315**, 31–35.
- Pačes T. (1986) Weathering rates of gneiss and depletion of exchangeable cations in soils under environmental acidification. *J. Geol. Soc. London* **143**, 673–677.

- Peters N. (1984) *Evaluation of Environment Factors Affecting Yields of Major Dissolved Ions of Streams in the United States; USGS Water Supply Pap.* 2228.
- Peters N. E. and Leavesley G. H. (1994) Biotic and abiotic processes controlling water chemistry during snowmelt at Rabbit Ears Pass, Rocky Mountains, Colorado, USA. *Water, Air, Soil Pollution* **79**, 171–190.
- Probst A., Viville D., Fritz B., Ambroise B., and Damrinc E. (1992) Hydrochemical budgets of a small forested granitic catchment exposed to acid deposition: The Strengbach Catchment case study (Vosges Massif, France). *Water, Air, Soil Pollution* **62**, 337–347.
- Reddy M. M. (1988) A small alpine basin budget: Front Range, Colorado. In *International Mountain Watershed Symp., Subalpine Processes and Water Quality* (ed. I. G. Poppoff et al.); *Tahoe Resource Conservation District, South Lake Tahoe, California*, pp. 370–385.
- Reynolds R. C. and Johnson N. M. (1972) Chemical weathering in a temperate glacial environment of the Northern Cascade Mountains. *Geochim. Cosmochim. Acta* **36**, 537–544.
- Schlinder D. W., Newbury R. W., Beaty K. G., and Cambell P. (1976) Natural water and chemical budgets for a small Precambrian Lake Basin in Central Canada. *J. Fish. Res. Board Canada* **33**, 2526–2543.
- Shimada Y., Ohte N., Tokuchi N., and Suzuki M. (1993) A dissolved silica budget for a temperate forested basin. In *Tracers in Hydrology; IAHS Publ.* 215, pp. 79–88.
- Siegel D. I. and Pfannkuch H. O. (1984) Silicate dissolution influence on Filson Creek chemistry, northeastern Minnesota. *GSA Bull.* **95**, 1446–1453.
- Skartveit A. (1981) Relationships between precipitation chemistry, hydrology and runoff acidity. *Nordic Hydrol.* **1981**, 65–80.
- Stahr K., Zottl H. W., and Hadrich F. (1980) Transport of trace elements in the ecosystems of the Barhalde watershed in the southern Black Forest. *Soil Sci.* **130**, 217–224.
- Stallard R. F. (1992) Tectonic processes, continental freeboard, and the rate controlling step for continental denudation. In *Global Biogeochemical Cycles* (ed. S. S. Butcher et al.), pp. 93–121. Academic.
- Stallard R. F. and Edmond J. M. (1983) Geochemistry of the Amazon: 2. The influence of the geology and weathering environment on the load. *J. Geophys. Res.* **88**, 9671–9688.
- Stauffer R. E. and Wittchen B. D. (1991) Effects of silicate weathering on chemistry in a forested, upland, felsic terrain of the USA. *Geochim. Cosmochim. Acta* **55**, 3253–3271.
- Stednick J. D. (1981) Hydrochemical balance of an alpine watershed in southeast Alaska. *Arctic Alpine Res.* **13**, 431–438.
- Sverdrup H. U. (1990) *The Kinetics of Base Cation Release Due to Chemical Weathering*. Lund Univ. Press, Sweden.
- Swank W. T. and Waide J. B. (1988) Characterization of baseline precipitation and stream chemistry and nutrient budgets for control watersheds. In *Forest Hydrology and Ecology at Coweeta* (ed. W. T. Swank and D. A. Crossley Jr.), pp. 57–79. Springer-Verlag.
- Velbel M. A. (1990) Influence of temperature and mineral surface characteristics on feldspar weathering rates in natural and artificial systems: A first approximation. *Water Res. Res.* **26**, 3049–3053.
- Velbel M. A. (1993a) Temperature dependence of silicate weathering in nature: How strong of a negative feedback on long term accumulation of atmospheric CO₂ and global greenhouse warming? *Geology* **21**, 1059–1062.
- Velbel M. A. (1993b) Constancy of silicate-mineral weathering-rate ratios between natural and experimental weathering: Implications for hydrologic control of differences in absolute rates. *Chem. Geol.* **105**, 89–99.
- Velbel M. A. (1994) Interactions of ecosystem processes and weathering processes in Solute Modelling in Catchment Systems (ed. S. Trudgill). Wiley (in press).
- Volk T. (1987) Feedbacks between weathering and atmospheric CO₂ over the last 100 million years. *Amer. J. Sci.* **287**, 763–779.
- Walker J. C. G., Hays P. B., and Kasting J. F. (1981) A negative feedback mechanism for the long-term stabilization of the Earth's temperature. *J. Geophys. Res.* **86**, 9776–9782.
- White A. F. et al. (1992) A three million year weathering record for a soil chronosequence developed in granitic alluvium, Merced, California, USA. In *Proc. 7th Intl. Symp. Water Rock Interaction* (ed. Y. K. Kharaka and A. S. Maest), pp. 607–610.
- White A. F., Blum A. E., Schulz M. S., Peterson M., and Hardin J. W. (1994) Chemical weathering in a soil chronosequence: Solid state weathering rates. *Geochim. Cosmochim. Acta* (in press).
- Williams M. W., Melack J. M., and Everson D. A. (1993) Export of major ionic solutes from two sub-alpine watersheds before and after fire. *Trans. Amer. Geophys. Union* **74**, 258.
- Wright R. F. (1983) Input-output budgets at Langtjern, a small acidified lake in southern Norway. *Hydrobiologia* **101**, 1–12.
- Wright R. F. and Johannessen M. (1980) Input-output budgets of major ions at gauged catchments in Norway. *Proc. Conf. Ecol. Impact Acid Precip., SNSF Proj. Norway*, pp. 250–251.
- Yuretic R. F. and Batchelder G. L. (1988) Hydrochemical cycling and chemical denudation in the Fort River Watershed, Central Massachusetts: An appraisal of mass-balance approaches. *Water Res. Res.* **24**, 105–114.
- Yuretic R., Knapp E., and Irvine V. (1993) Chemical denudation and weathering mechanisms in central Massachusetts, USA. *Chem. Geol.* **107**, 345–347.
- Zeman L. J. (1978) Mass balance model for calculation of ionic input loads in atmospheric fallout and discharge from a mountainous basin. *Hydrol. Sci. Bull.* **23**, 103–117.

Effects of climate on chemical weathering in watersheds

White, Art F; Blum, Alex E

01	Nicholas Gubbins	Page 1
10/9/2020 16:34		
02	Nicholas Gubbins	Page 1
10/9/2020 16:34		
03	Nicholas Gubbins	Page 1
10/9/2020 16:34		
04	Nicholas Gubbins	Page 1
10/9/2020 16:34		
05	Nicholas Gubbins	Page 1
10/9/2020 16:34		
06	Nicholas Gubbins	Page 1
10/9/2020 16:34		
07	Nicholas Gubbins	Page 1
10/9/2020 16:34		
08	Nicholas Gubbins	Page 1
10/9/2020 16:34		
09	Nicholas Gubbins	Page 3
10/9/2020 18:42		
10	Nicholas Gubbins	Page 7
10/9/2020 18:42		

11	Nicholas Gubbins	Page 7
10/9/2020 18:42		
12	Nicholas Gubbins	Page 9
10/9/2020 18:42		
13	Nicholas Gubbins	Page 10
10/9/2020 18:42		
14	Nicholas Gubbins	Page 10
10/9/2020 18:42		
15	Nicholas Gubbins	Page 10
10/9/2020 18:42		
16	Nicholas Gubbins	Page 11
10/9/2020 18:42		
17	Nicholas Gubbins	Page 12
8/7/2021 17:48		
18	Nicholas Gubbins	Page 12
8/7/2021 17:49		
19	Nicholas Gubbins	Page 15
10/9/2020 18:42		
20	Nicholas Gubbins	Page 16
10/9/2020 18:42		
21	Nicholas Gubbins	Page 16
10/9/2020 18:42		
22	Nicholas Gubbins	Page 16
8/7/2021 17:51		

10/9/2020 18:42

10/9/2020 18:42

10/9/2020 18:42

10/9/2020 18:42